



**HAL**  
open science

# The transition from Pyrenean shortening to Gulf of Lion rifting in Languedoc (South France) - A tectonic sedimentation analysis

Michel Seranne, Renaud Couëffé, Michel Séranne, Céline Baral, Justine Villard

## ► To cite this version:

Michel Seranne, Renaud Couëffé, Michel Séranne, Céline Baral, Justine Villard. The transition from Pyrenean shortening to Gulf of Lion rifting in Languedoc (South France) - A tectonic sedimentation analysis. Bulletin de la Société Géologique de France, 2021, 192, pp.27. 10.1051/bsgf/2021017 . hal-03358027

**HAL Id: hal-03358027**

**<https://hal.science/hal-03358027>**

Submitted on 29 Sep 2021

**HAL** is a multi-disciplinary open access archive for the deposit and dissemination of scientific research documents, whether they are published or not. The documents may come from teaching and research institutions in France or abroad, or from public or private research centers.

L'archive ouverte pluridisciplinaire **HAL**, est destinée au dépôt et à la diffusion de documents scientifiques de niveau recherche, publiés ou non, émanant des établissements d'enseignement et de recherche français ou étrangers, des laboratoires publics ou privés.

1 *Bulletin de la Société Géologique de France, "Orogen lifecycle: learnings and perspectives from Pyrenees,*  
2 *Western Mediterranean and analogues".*  
3 *SGF - Earth Sciences Bulletin, 192, 10.1051/bsgf/2021017 – 2021.*

4  
5

6

7 **The transition from Pyrenean shortening to Gulf of Lion**  
8 **ripping in Languedoc (South France) – A tectonic-**  
9 **sedimentation analysis.**

10

11 Michel Séranne<sup>1\*</sup>, Renaud Couëffé<sup>2</sup>, Eglantine Husson<sup>2</sup>, Céline Baral<sup>1</sup>, Justine Villard<sup>1</sup>

12

13 (1) Géosciences Montpellier, CNRS - Université de Montpellier - Université de Guadeloupe,  
14 MONTPELLIER, France

15 (2) BRGM, GeoResources Division, ORLEANS, France

16

17

18 □ Corresponding author.

19 E-mail address: michel.seranne@umontpellier.fr (M. Séranne)

20 Orcid# 0000-0001-5862-2003

21

22

23

24

25 **Abstract:**

26 The pyrenean orogen extended eastward, across the present-day Gulf of Lion margin. The  
27 late or post-orogenic dismantling of this orogen segment, contemporaneous with ongoing  
28 shortening in the Spanish Pyrenees, is still debated. Understanding the transition between the  
29 two geodynamic events requires to document the precise timing of the succession of the  
30 tectonic processes involved. We investigate the superposition of rifting structures over  
31 pyrenean thrusts and folds in the onshore Languedoc. Compilation and reassessment of the  
32 regional chronostratigraphy, in the light of recent biostratigraphic dating and new mapping of  
33 Paleogene basins, lead to date the transition to the Priabonian. Tectonic-sedimentation  
34 relationship in the Eocene to Oligocene depocentres are analysed in surface exposures as  
35 well as in seismic reflection surveys. Bed-to bed mapping allowed us to: i) characterise an  
36 intermediate sequence of Priabonian age, bounded at the base and the top by unconformities;  
37 ii) evidence syn-depositional deformation within the Priabonian; iii) define the axes of  
38 Priabonian deformation. Interpretation of seismic reflection profiles, across the onshore basins  
39 covered by syn- and post-rift sequences, reveal the existence of an intermediate sequence  
40 displaying similar features, and that is correlated to the Priabonian. Syn-depositional  
41 deformation of some Priabonian basins correspond to extensional structure, whereas  
42 neighbouring, contemporaneous basins, reveal compressional deformation. The distribution of  
43 such apparently conflicting observations across the studied area provides evidence for left-  
44 lateral strike-slip deformation between two major regional faults (Cévennes and Nîmes faults).  
45 Left-lateral strike-slip along NE-trending faults accommodates E-W extension of the West  
46 European Rift (ECRIS) and part of the ongoing N-S shortening in the Central and Western  
47 Pyrenees. Priabonian clastic sedimentation and deformation in Languedoc witness the initial  
48 stages of the dismantling of the Languedoc-Provence Pyrenees, prior to Oligocene-Aquitania  
49 back-arc rifting.

50

51 **Keywords:**

52 **Pyrenees, Gulf of Lion, strike-slip basins, syn-depositional deformation, Priabonian**

53

54

55 **Résumé (français)**

56 L'orogène pyrénéen s'étendait vers l'est à l'emplacement actuel du Golfe du Lion.  
57 Contemporain de la poursuite de la compression dans les Pyrénées franco-espagnoles, le  
58 démantèlement tardi- ou post-orogénique de ce segment de l'orogène est encore mal compris.  
59 La compréhension de la transition entre l'orogénèse Pyrénéo-Provençale et le rifting du Golfe  
60 du Lion nécessite de préciser le calendrier des événements ainsi que la succession des  
61 différents processus tectoniques mis en jeu. Nous analysons la superposition des structures

62 du rifting sur les structures compressives Pyrénéennes exposées à terre, dans le Languedoc.  
63 Tout d'abord, nous compilons et révisons la chronostratigraphie régionale, à la lumière de  
64 datations postérieures à la publication des cartes au 1/50.000- du BRGM, et de la cartographie  
65 de plusieurs bassins paléogènes. Nous datons cette transition du Priabonien. Nous analysons  
66 les relations tectonique-sédimentation des dépocentres Eocène à Oligocène sur le terrain et  
67 en sismique réflexion. La cartographie banc-par-banc permet de : i) caractériser une séquence  
68 intermédiaire d'âge Priabonien encadrée par deux discordances, ii) mettre en évidence une  
69 déformation syn-dépôt dans le remplissage Priabonien, iii) définir les axes de la déformation  
70 priabonienne. L'interprétation de profils de sismique réflexion à travers les bassins paléogènes  
71 à terre, recouverts par les séries syn-et post-rift, révèle l'existence d'une séquence  
72 intermédiaire présentant des caractéristiques similaires et que nous corrélons avec le  
73 Priabonien. La déformation syn-dépôt de certains bassins est extensive, alors que dans des  
74 bassins voisins contemporains, elle est compressive. La distribution régionale de ces  
75 observations apparemment contradictoires est interprétée comme liée à un couloir de  
76 déformation en décrochement senestre entre les failles majeures des Cévennes et de Nîmes,  
77 d'orientation NE-SW. Ce décrochement accommode l'extension EW des rifts ouest-européens  
78 et contribue au raccourcissement N-S des Pyrénées franco-espagnoles, toujours actif au  
79 Priabonien. La sédimentation syn-tectonique clastique du Priabonien du Languedoc enregistre  
80 les premiers stades du démantèlement de la chaîne pyrénéo-provençale, plusieurs millions  
81 d'années avant l'initiation de l'extension d'arrière-arc.

82

83 **Mots-clé:**

84 **Pyrénées, Golfe du Lion, bassins sur décrochement, déformation syn-sédimentaire,**  
85 **Priabonien,**

86



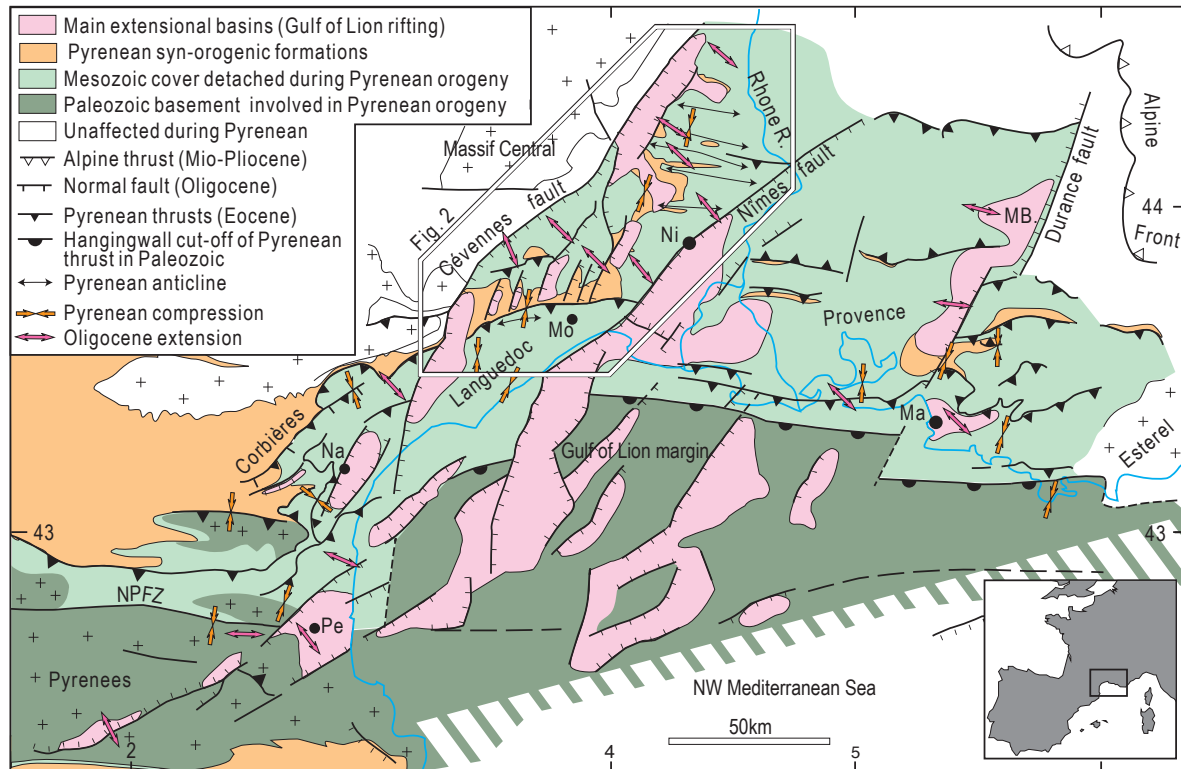
## 87 **1. Introduction**

88

89 The Pyrenean orogen results from the inversion of Mesozoic extensional basins, mostly  
90 formed during Mid-Cretaceous rifting and mantle denudation (Chelalou et al., 2016; Cochelin  
91 et al., 2018; Lagabrielle and Bodinier, 2008; Lagabrielle et al., 2010; Ternois et al., 2019 ;  
92 Tugend et al., 2014; Vergés and Garcia-Senz, 2001). The orogenic shortening was  
93 accommodated in the upper crust by reactivation of the inherited Cretaceous extensional  
94 faults, as thrust faults (Debroas, 1990), while the middle crust and exhumed mantle were  
95 subducted beneath the European crust (Teixell et al., 2018; Teixell et al., 2016). The orogen  
96 extended eastwards (Ford and Vergés, 2020), in Corbières (Lamotte et al., 2002; Viillard,  
97 1987), Languedoc (Arthaud and Laurent, 1995) and southern Provence (Bestani et al., 2015;  
98 Lacombe and Jolivet, 2005), across the present-day Gulf of Lion (Arthaud and Séguret, 1981;  
99 Gorini et al., 1994). It was later dismantled in Oligocene time to give way to the Gulf of Lion  
100 rifted margin (Arthaud et al., 1981; Arthaud and Séguret, 1981; Gorini et al., 1994; Guennoc  
101 et al., 2000; Lacombe and Jolivet, 2005; Mascle and Vially, 1999; Mauffret and Gorini, 1996;  
102 Séranne, 1999; Séranne et al., 1995). In the onshore Corbières area, upper crust extension is  
103 characterised by “negative inversion” of the Pyrenean thrusts, associated with deposition of  
104 Oligocene-Aquitainian syn-rift sediments in the hanging-wall (Gorini et al., 1991). The crustal  
105 roots of the Pyrenees disappear eastwards (Chevrot et al., 2018) and the orogen brutally gives  
106 way to the Gulf of Lion rift and margin, within only tens of kilometres (Jolivet et al., 2020;  
107 Mauffret et al., 2001). Although documented both onshore and offshore, tectonics and  
108 kinematics of the superimposition of Pyrenean structures by later rifting (Fig. 1) remains  
109 incompletely understood. Transition of the compression to extension could be driven by  
110 collapse of the elevated mountain range (Séranne et al., 1995), it could be related to the  
111 southern propagation of the European Cenozoic Rift System (ECRIS) (Dèzes et al., 2004), or  
112 to the onset of back-arc extension due to the NW-dipping subduction roll-back of the old  
113 Tethyan lithosphere (Jolivet et al., 2020; Séranne, 1999). Better constraints on tectonics and  
114 precise timing of the transition from the Pyrenean orogeny to the Gulf of Lion rifting are needed  
115 in order to better understand the origin and driving mechanism of the transition between the  
116 two major geodynamics events. Such data are also needed to constrain paleotectonic  
117 restorations (e.g. (Bestani et al., 2015; Christophoul et al., 2016), and kinematic  
118 reconstructions of the Mediterranean (e.g. (Romagny et al., 2020).

119 Since most of the collapsed orogen is presently buried beneath the thick Neogene sequence  
120 of the Gulf of Lion margin, the onshore Languedoc provides the only geological outcrops that  
121 are relevant to address this question. There, the rare available stratigraphic data suggested  
122 that the Pyrenean orogeny lasted until “early Oligocene”, as reported on the Saint-Martin-de-  
123 Londres 1/50.000-scale geological map (Philip et al., 1978), while rifting took place in the late

124 Rupelian according to the Montpellier map (Andrieux et al., 1971). Consequences of such a  
 125 short delay implies: i) that Pyrenean compression was polyphase, including a last compressive  
 126 phase, following a Late Eocene period of tectonic quiescence, and ii) rifting interrupted folding  
 127 and thrusting, with no transition.

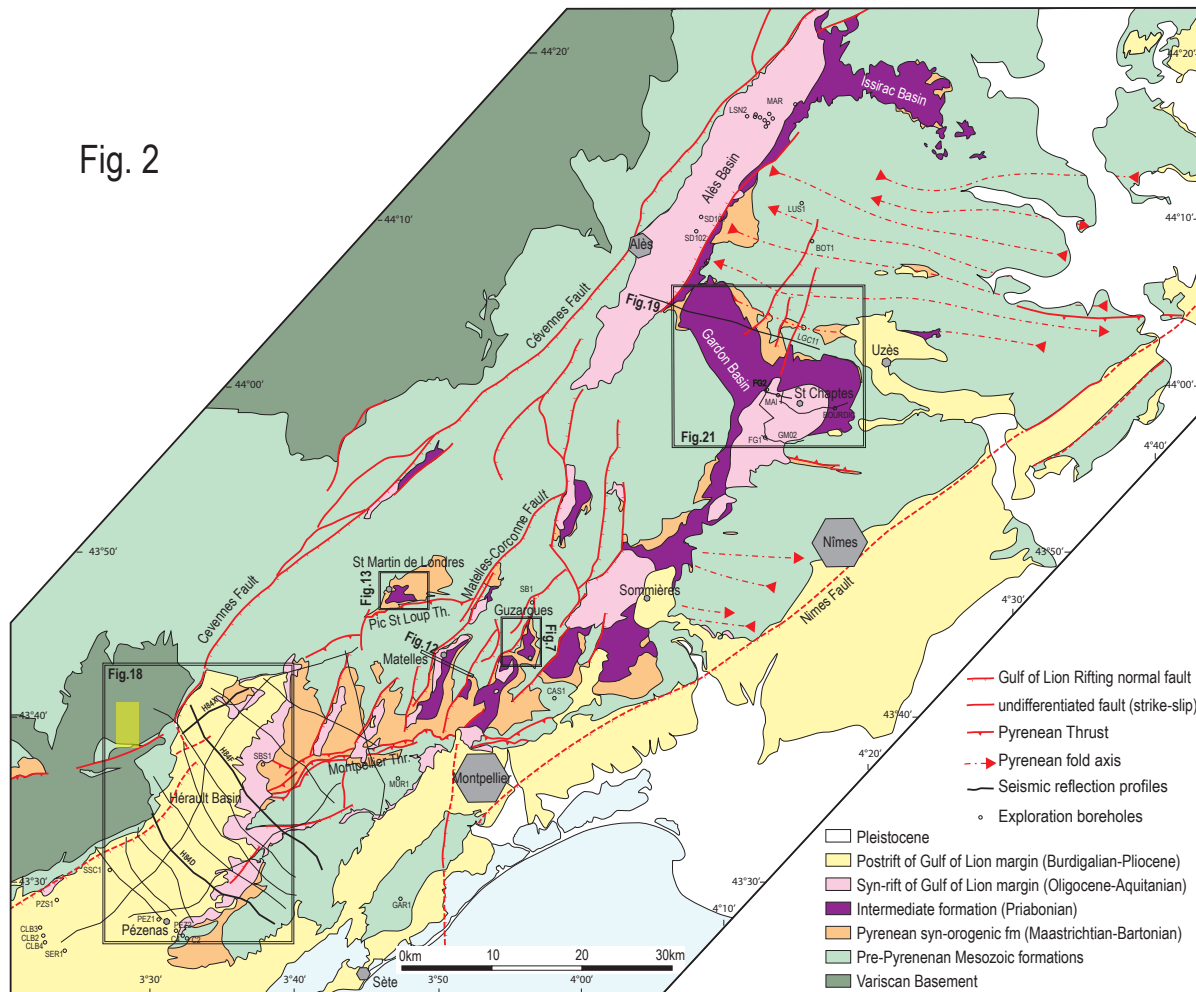


128  
 129 **Fig. 1:** Structural map southern France showing the relation between the Pyrenees and Gulf of Lion  
 130 margin; modified from (Séranne et al., 1995). Na: Narbonne, Pe: Perpignan, Mo: Montpellier, Ma:  
 131 Marseille. Directions of Pyrenean shortening from (Arthaud and Laurent, 1995), (Gaviglio and Gonzales,  
 132 1987; Lacombe et al., 1992; Lamotte et al., 2002) and Oligocene extension from : (Arthaud et al., 1977;  
 133 Benedicto, 1996; Hippolyte et al., 1993).

134  
 135 In this paper, we examine five Paleogene basins located in Languedoc, which developed at  
 136 the front of the Eocene external thrusts of the Pyrenean belt and onshore of the Gulf of Lion  
 137 passive margin. The main objective of this contribution is to document, thanks to the revision  
 138 of available biostratigraphic data and to detailed sedimentological, tectonic and seismic  
 139 analyses, the key period of the transition between the last stages of Pyrenean orogenic  
 140 (mountain building) events and the earliest stages of rifting associated with the opening of the  
 141 Gulf of Lion. We aim at constraining the tectonic setting associated with the deposition of  
 142 Priabonian continental units by analysing the tectonic-sedimentation relationships in 5  
 143 distinctive basins (Fig. 2). Analyses are based on field observations (Guzargues, Les-Matelles,  
 144 Saint-Martin-de-Londres basins) and subsurface data (Hérault and Saint-Chaptes Gardon  
 145 basins). This study also relies on: i) new original investigation in the Guzargues basin, ii)

146 reappraisal of published works in Les-Matelles and Saint-Martin-de-Londres basins (the latter  
 147 involving additional mapping), and iii) the interpretation of ancient (1983-1992) seismic profiles  
 148 tied to boreholes data in the Hérault and Saint-Chartes Gardon basins.

Fig. 2



149  
 150 **Fig. 2:** Simplified geological map of Languedoc, in the northern foreland of the Provence-Pyrenees fold  
 151 and thrust belt. See location in the regional structural framework of Fig.1. Priabonian basins according  
 152 to the present study, in some areas, stratigraphic attributions are different from the BRGM 1/50.000-  
 153 scale geological maps (see text for explanation). Subsurface data used in the study is indicated fine  
 154 black lines (seismic) and open circles (boreholes); seismic profiles shown in this contribution are in  
 155 bolder black line. Location of detailed maps and sections is shown with double black line frames.

156

## 157 2. Regional geological setting

158

### 159 2-1 Location of the studied area within the Pyrenean orogen

160

161 Languedoc, in the south of France, is located between the Variscan basement of the Massif  
 162 Central and the shores of the Mediterranean Sea; it links the Pyrenees (in the SW) to the Alps  
 163 (to the NE), across the Rhône Valley (Fig. 1). Together with the Corbières, Languedoc forms

164 a segment of the north foreland of the Pyreneo-Provençal fold and thrust belt (Arthaud and  
165 Séguret, 1981; Bestani et al., 2015).

166 The Paleozoic (Variscan) basement is exposed in the Massif Central to the NW, in the Maure  
167 and Esterel massifs to the east. To the south, the basement has been reactivated during the  
168 Late Cretaceous to Eocene Pyrenean orogeny. It is exposed in the Pyrenees and buried  
169 beneath the thick Neogene sequences of the Gulf of Lion margin (Arthaud and Séguret, 1981;  
170 Gorini et al., 1994; Guennoc et al., 2000) (Fig. 1). Onshore, the Variscan basement is  
171 unconformably covered by Mesozoic sequence, including at the base variable amounts of  
172 Triassic detritals and evaporites (Debrand-Passard and Courbouleix, 1984), which have been  
173 used as decollement level during later tectonic phases. The Jurassic through to Neocomian  
174 marine marls and carbonates were deposited during the Tethyan rifting and subsequent  
175 thermal subsidence, controlled by NE-trending normal faults such as the Cévennes, Nîmes  
176 and Durance faults. Thickness of the Jurassic increases southeastwards from the Cévennes  
177 fault (less than 1,5km), and maximum subsidence is recorded in the hanging-wall of the Nîmes  
178 Fault, where seismic profiles show up to 10km of Trias to Neocomian sequences (Le Pichon  
179 et al., 2010; Séguret et al., 1997).

180 This Mesozoic sedimentary cover has been folded and thrust in the Pyrenean foreland,  
181 detached over Triassic decollement. Thick-skinned thrusting presumably occurred close to the  
182 present day shoreline (Arthaud and Séguret, 1981; Lacombe and Jolivet, 2005; Séranne et al.,  
183 1995 ), The style of the thrust and fold belt is mostly controlled by the thickness of the detached  
184 Mesozoic sedimentary cover (Arthaud and Laurent, 1995): north-verging, EW-oriented thrusts  
185 dominate areas of thin cover ( $\leq 2,5$  to 3 km) whereas thicker cover developed series of E-W  
186 folds. Combined thin- and thick-skinned shortening exceed 20km in the Languedoc (Arthaud  
187 and Laurent, 1995) and 40km in the Provence segment of the orogen (Bestani et al., 2016;  
188 Bestani et al., 2015). The Pyrenees-Provence fold and thrust belt is segmented by NE- to NNE-  
189 trending faults which separate areas of distinct structural styles and amounts of shortening.  
190 Left-lateral strike-slip along the Cévennes Fault accommodated shortening of its hanging-wall  
191 while the NW footwall remained mostly undeformed during the Pyrenean orogeny (Arthaud  
192 and Laurent, 1995). In Provence, the Durance Fault separates thin- and thick-skinned  
193 Pyrenean deformation (Bestani, 2015; Bestani et al., 2016).

194

## 195 ***2-2. Location of the studied area within the Gulf of Lion rift and passive margin***

196

197 The studied area is affected by NE-trending normal faults bounding syn-rift Oligocene basins  
198 (Fig. 2). At least, some of these faults - if not all - are reactivated previous Pyrenean left-lateral  
199 strike-slips faults (i.e. the Cévennes fault, Matelles Fault (Mattauer, 2002). Seismic reflection  
200 profiling has shown that, during Oligocene rifting, such faults detached in the Triassic

201 decollement (Benedicto, 1996; Benedicto et al., 1999; Husson, 2013; Sanchis and Séranne,  
202 2000). The onshore syn-rift basins NW of the Nîmes Fault were formed by thin-skinned  
203 extensional tectonics (Séranne, 1999). The basement-cover decollement ramps down in the  
204 Nîmes basement fault (Benedicto et al., 1996) and into the basement ramp of the Montpellier  
205 thrust to the south and southeast of the study area.

206

### 207 **3. Revised chronology of events**

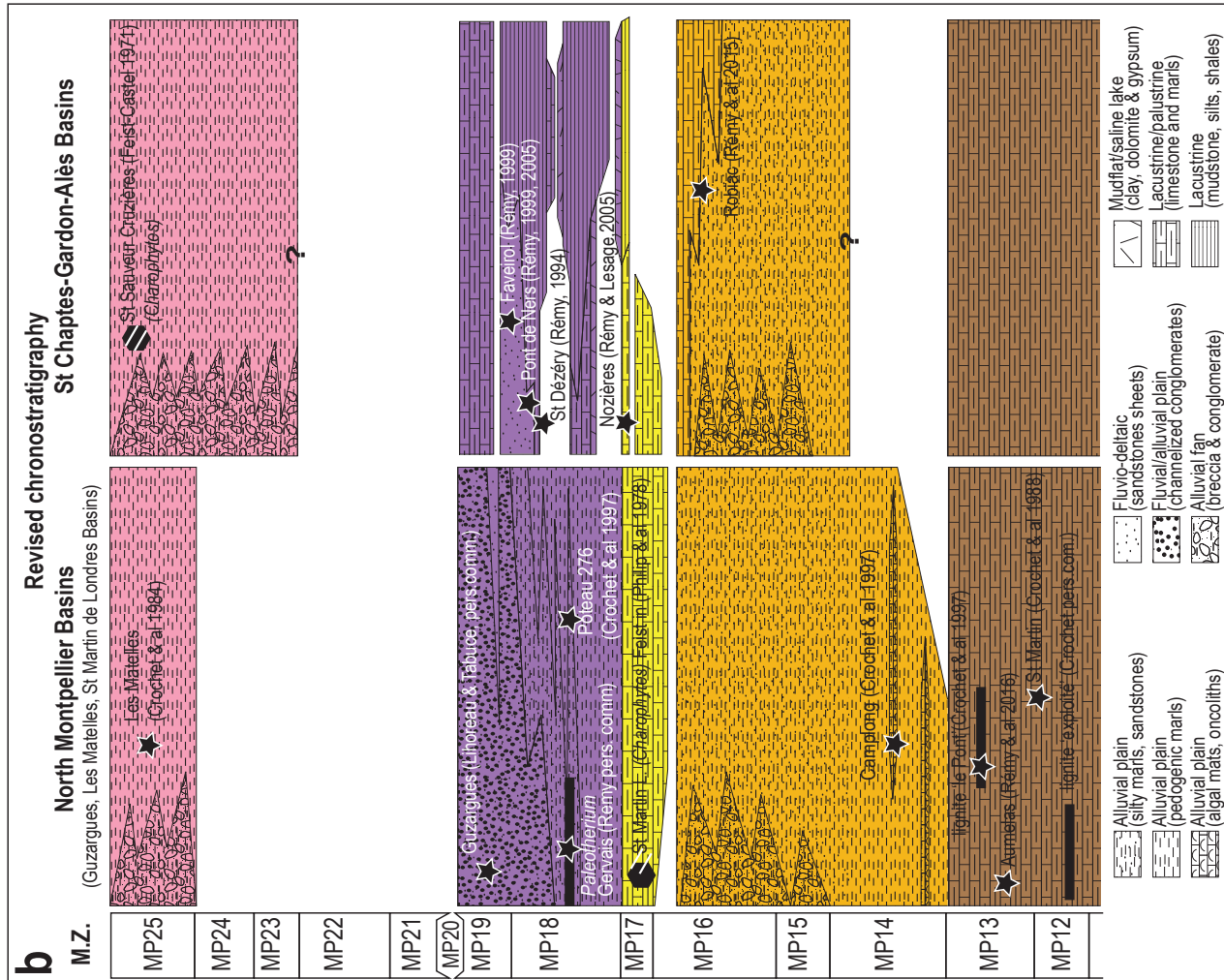
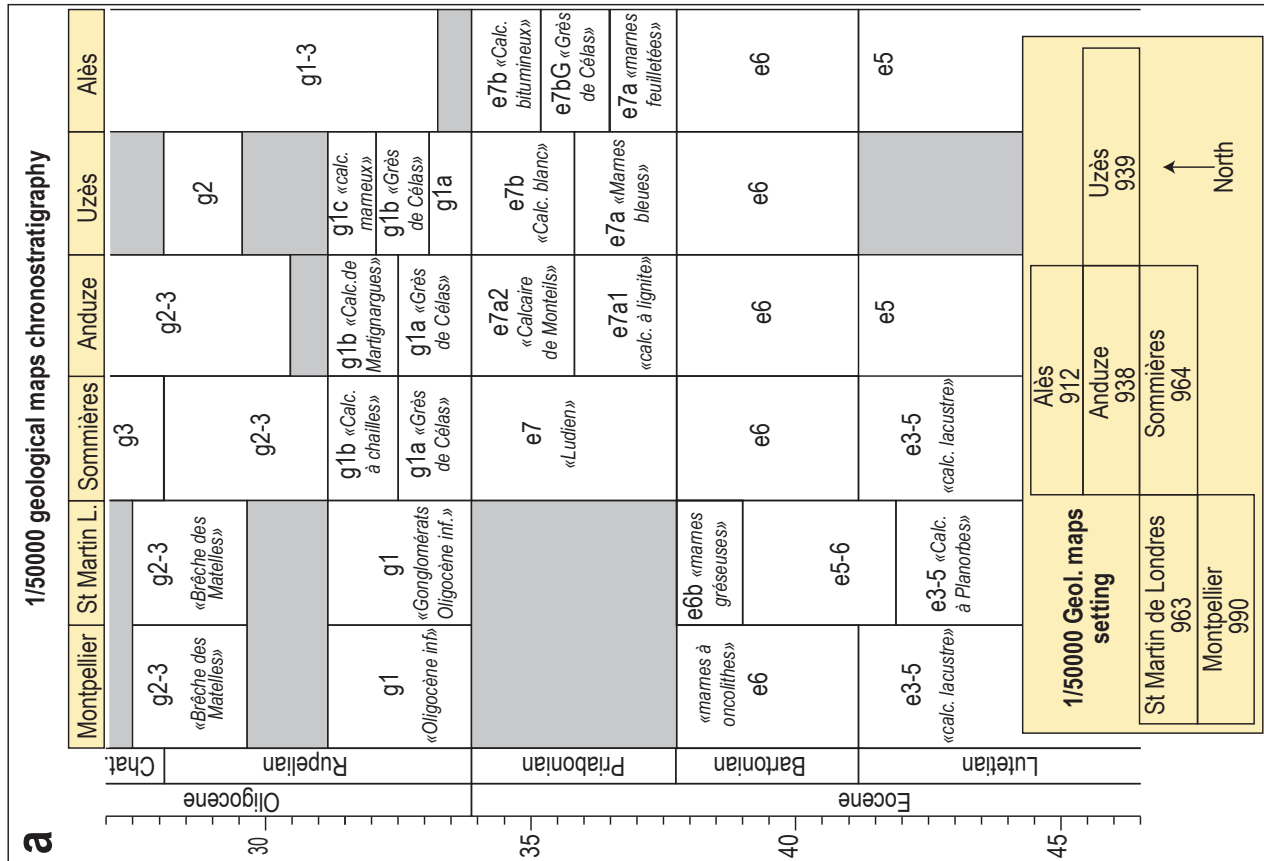
208

209 The chronology of the transition between Pyrenean orogeny and the Gulf of Lion rifting is still  
210 discussed. The stratigraphy of the 1/50.000-scale geological maps of the study area is  
211 confusing: all maps are consistent in identifying the Bartonian (e6) as a Pyrenean syn-tectonic  
212 sequence, but they greatly diverge in dating the end of the orogeny and the onset of the rifting.  
213 The comparison of stratigraphy of the adjacent maps of the study area reveals contradicting  
214 ages for identical and spatially continuous formations (Fig. 3 a).

215 Another inconsistency arises from the outstanding question: what was the geodynamic  
216 context during the time interval between the Pyrenean syn-orogenic deposits and the syn-rift  
217 formations? Adjacent maps carry contradicting interpretations: the « g1 » is a continuity of the  
218 syn-orogenic Bartonian on the Saint-Martin-de-Londres map (Philip et al., 1978), whereas the  
219 Montpellier map correlates the « g1 » with the early stages of the Gulf of Lion rifting (Andrieux  
220 et al., 1971).

221 The mammalian reference levels developed for the Paleogene continental record of Europe  
222 (Sigé and Legendre, 1997), allowed to improve the stratigraphy and to revise the tectonic  
223 agenda of the area, especially around the transition from orogeny to rifting. Figure 3b uses  
224 chronology of (Vandenberghe et al., 2012) and mammal reference levels of (Aguilar et al.,  
225 1997).

226 The age of the lacustrine limestone was defined as Lutetian or slightly older. In the Pic-Saint-  
227 Loup foreland, fauna allowed to place this formation between MP12 and MP13 reference levels  
228 of the mammal reference levels (Crochet et al., 1988). In different localities of Les-Matelles  
229 basin, several lignite beds provided a diversified fauna, which correlates with the Lutetian  
230 (MP13) (Crochet et al., 1997). A distinctive marly facies including 1 to 20cm diameter  
231 oncolithes, occurs at the top. It has yielded fauna ascribed to the MP14 reference level  
232 (Crochet et al., 1997) of latest Lutetian age. This facies passes southwards and upwards to  
233 the Bartonian syn-orogenic breccia, exposed along the Montpellier thrust (Andrieux et al.,  
234 1971). In the Sommières and Saint-Chaptes basins the reference sites of Robiac provided a  
235 late Bartonian age for the latest Pyrenean syn-tectonic formations (Remy, 2015).





237 **Fig. 3 a:** Correlation chart of the Eocene to Oligocene interval, and inferred ages, according to the  
 238 BRGM 1/50.000-scale geological maps of the study area. The inset in the lower part gives the position  
 239 of the BRGM 1/50.000-scale geological maps. **b:** Revised chronostratigraphy of the basins north of  
 240 Montpellier (covered by the geological maps of Montpellier, St Martin-de-Londres and part of Sommières  
 241 and Anduze) and of the St Chaptes-Gardon basins (maps of Alès and part of Anduze and Uzès). This  
 242 is based on new mapping of the Paleogene basins (this study) and on the compilation of biostratigraphy  
 243 data, including recent discoveries of mammal fossils (references in the figure and in the text).  
 244 Biostratigraphy scale according to mammal reference levels (M.Z.). Black stars and black hexagons  
 245 correspond to mammal and charophyte sites, respectively. Simplified lithology of the formations is  
 246 indicated. Colour code as in the following maps and sections of the Paleogene basins analysed in this  
 247 study. White areas corresponds to non-depositional and erosional hiatuses; the Priabonian interval from  
 248 St Chaptes-Gardon-Alès basins is documented in (Lettéron et al., 2018).

249

250 They pass upward to continental marls and limestones dated to the Bartonian-Priabonian  
 251 transition (MP17) (Remy, 2015; Rémy and Lesage, 2005). In the Saint-Martin-de-Londres  
 252 basin, similar lithologies correspond to time equivalent, as suggested by charophytes (Feist in  
 253 Philip et al., 1978).

254 The overlying formation mapped as « g1 » in Les-Matelles basin, displays polygenic  
 255 conglomerates and sandstones within yellow marls and silts, including several lignite beds.  
 256 They are interpreted as alluvial plain deposits (Benedicto et al., 1999; Egerton, 1996). The age  
 257 of this formation was subjected to discussion due to the controversial location of the discovery  
 258 by Gervais, in the late XIX<sup>th</sup> Century, of a *Lophiodon* skull (see review in (Hartenberger et al.,  
 259 1969). Reappraisal of the specimen, exhumed from Lyon university collections by J. A. Remy  
 260 (*personal communication*), relates the specimen to MP 18 (middle Priabonian). Another  
 261 *Lophiodon* specimen has recently been discovered in the correlative « g1 » formation in the  
 262 Guzargues basin, and has been related to the MP19 reference level (R. Tabuce and F.  
 263 Lihoreau, *personal communication*). The age of this conglomerate formation is therefore  
 264 attributed to the Priabonian. As first suggested by (Andrieux et al., 1971), it is correlated with  
 265 the detrital continental formation « Grès de Célas » of upper Priabonian, in the Sommières and  
 266 Saint-Chaptes - Gardon basins, northeast of the study area, which spans the MP18 to MP19  
 267 (Rémy, 1985; Remy and Fournier, 2003; Rémy and Lesage, 2005).

268 At Les-Matelles and Saint-Vincent-de-Barbeyrargues localities, yellow to orange marls  
 269 interfingering with syn-rift breccia, contain charophytes (Grambast, 1962), teeth of small  
 270 mammals (Thaler, 1962) and gastropods (Rey, 1962) that yielded mid- to late- «Stampian»  
 271 age, which corresponds to the Late Rupelian. This age was later confirmed by the discovery  
 272 of small mammals in Les-Matelles half-graben, that relate to MP25 mammal scale (Crochet,  
 273 1984). In addition, breccia pipes and dykes of intracontinental alkaline basalt, that intrude  
 274 Lutetian and Priabonian formations, were dated 24 to 28 Ma (Gastaud et al., 1983), and have

275 been related to the Late Rupelian rifting event (Dautria et al., 2010; Séranne, 1999). In the  
276 northern basins, this unconformable formation has not yet provided mammal remains, but  
277 Charophytes from the alluvial environments of Saint-André-de-Cruzières in the north of Alès  
278 Basin yielded an Oligocene age (Feist-Castel, 1971).

279 Reappraisal of ancient specimens and new discoveries thus indicate that the sequence made  
280 of marls, sandstones beds and polygenic channelized conglomerates, which is exposed in  
281 separated basins across the study area, belongs to the same interval, dated to the Priabonian.  
282 In particular, the fluvial conglomerate and yellow sandy marls (reported on the published maps  
283 as “g1”, Fig. 3a), correlate with, and are the proximal equivalent of the lacustrine delta  
284 sandstones “Grés de Célas” of the Alès Basin (Lettéron et al., 2018). This formation is  
285 intermediate between the syn-orogenic Pyrenean (Bartonian) and the syn-rift (Late Rupelian)  
286 deposits. Furthermore, it is bounded by two marked angular unconformities, the upper one  
287 corresponding to a several-million-years hiatus.

288 In the following, we examine key field evidence in the north-Montpellier area (Guzargues, Les-  
289 Matelles and St-Martin-de-Londres basins, respectively) where the tectonic sedimentation  
290 relationships allow to characterise this intermediate formation. It can be interpreted as the  
291 record of the transition between the Pyrenean orogeny to the Gulf of Lion rifting.

292

#### 293 **4. Tectonic and sedimentation in the Guzargues Basin**

294

##### 295 ***4-1. Lithostratigraphy of Eocene deposits in the Guzargues area***

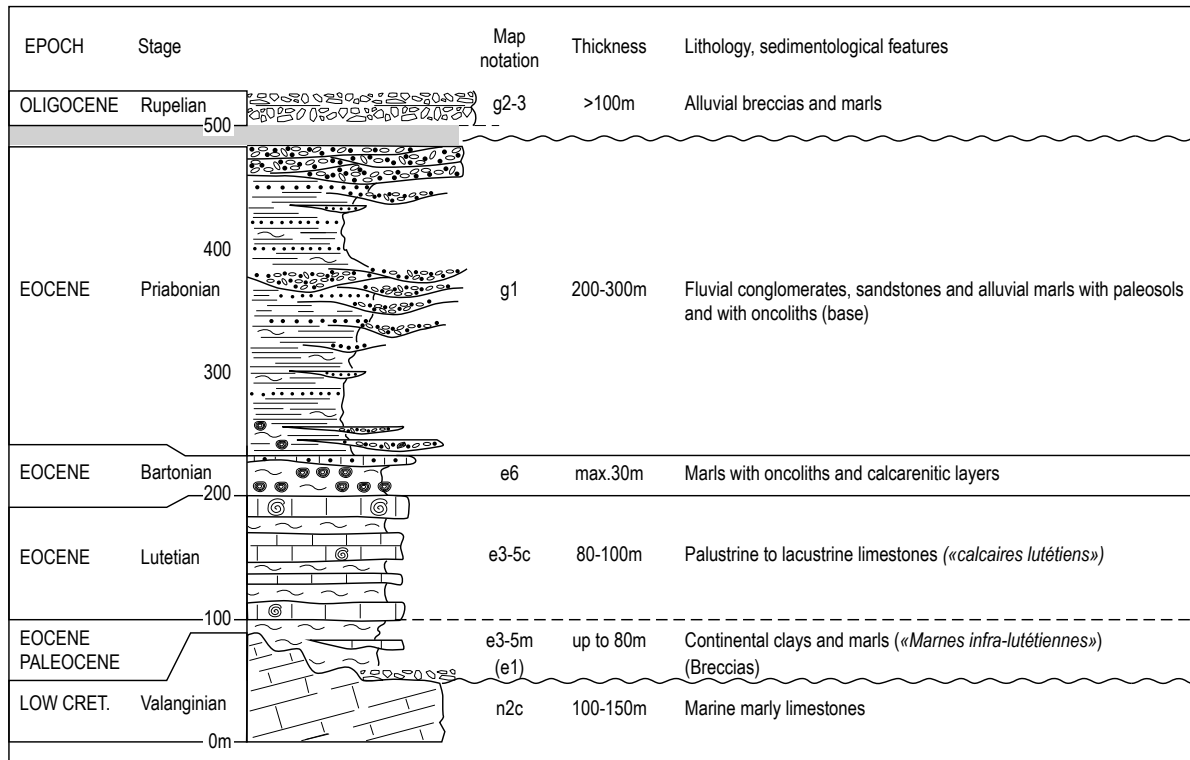
296

297 The Guzargues basin (Fig. 2) has not been the topic of any specific study and remains poorly  
298 documented. The Paleogene sedimentary succession contains 4 main lithological units  
299 representative of the regional geodynamic history since the early stages of the Pyrenean  
300 compression to the main rifting phase (Fig. 4). When possible, all of them were precisely  
301 mapped to analyse the geometrical relationships of Priabonian deposits with under- and  
302 overlying units.

303 (1) Paleocene to Lower Eocene facies are represented by fluvial marls with interbedded  
304 sandstones and palustrine limestones (“*Marnes infra-lutétiennes*”), only few tens of metres  
305 thick in the Guzargues area. They are usually correlated to alluvial fan syn-tectonic breccias,  
306 reworking the Jurassic succession at the front of the Montpellier thrust, and thus deposited  
307 during the early stages of the Pyrenean compression.

308





309

310 **Fig. 4:** Generalised lithostratigraphy of the Late Mesozoic and Paleogene in the Guzargues Basin and  
 311 immediate surrounding.

312

313 (2) Massive whitish Lutetian limestones, up to 100m thick in the area, form an easily  
 314 recognised, continuous unit displaying folds produced by late stages of the Pyrenean  
 315 compression.

316 (3) Lutetian limestones are conformably capped by a singular unit, up to 30m thick, made of  
 317 lacustrine to shallow marine, marly facies containing oncoliths and calcarenitic layers,  
 318 Bartonian in age.

319 (4) Topmost deposits of the Paleogene succession in the Guzargues area correspond to  
 320 Priabonian fluvial deposits showing alternations of conglomerates, sandstones and marls, up  
 321 to 300 m thick. Pebbles are supplied both from distant Pyrenean sources and from local  
 322 Mesozoic carbonates. These deposits rest unconformably above the Pyrenean folds consisting  
 323 of Lutetian to Bartonian units.

324 One kilometre to the south, the northern edge of the neighbouring Assas basin shows a  
 325 sedimentary unit of strong geodynamic significance, which is missing in the Guzargues basin.  
 326 Close to the Assas village, Oligocene breccias and marls, usually interpreted as syn-rift  
 327 deposits, unconformably overlie Priabonian continental facies.

328 Thus, the Priabonian deposits of the Guzargues basin, bounded below and above by  
 329 unequivocal syn-tectonic units, represent a key unit to study the transition between two main  
 330 regional geodynamic events.

331

332 **4-2. Sedimentological features of Priabonian deposits in the Guzargues basin**

333

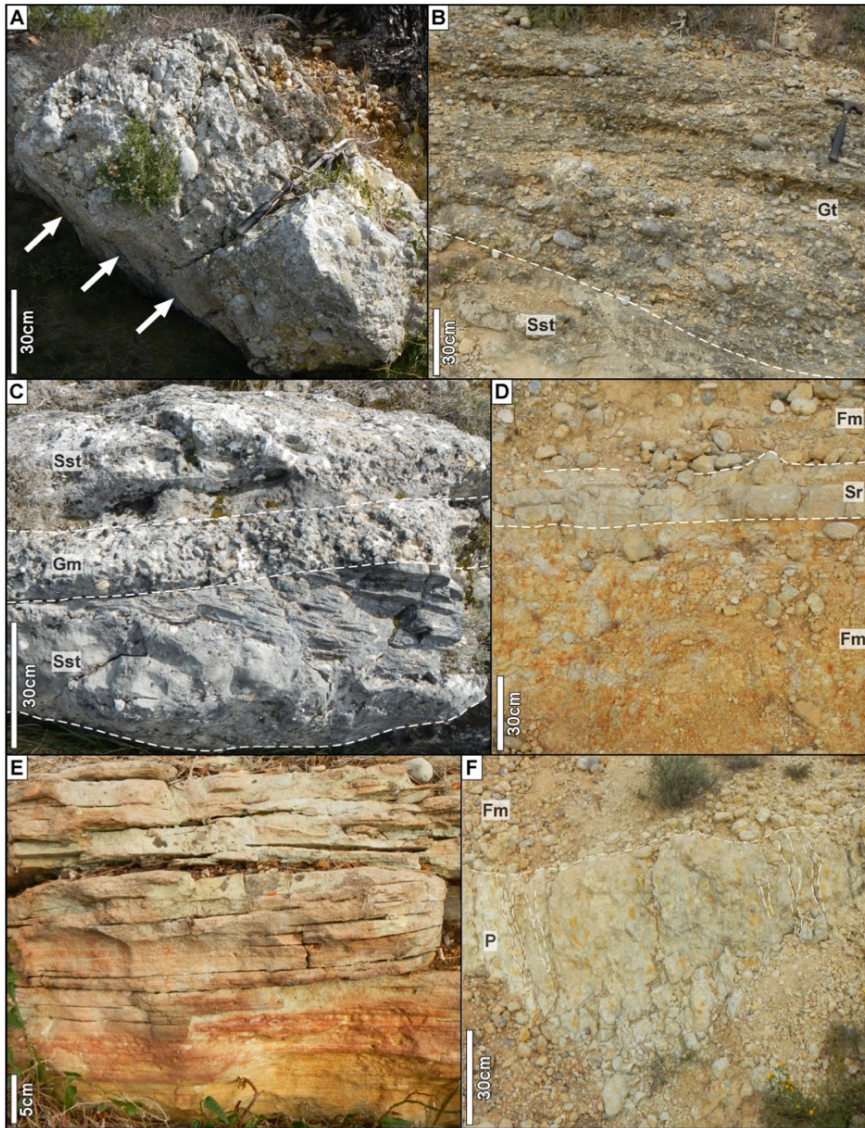
334 As observed in the 10 sections studied in the Guzargues basin, Priabonian deposits are  
335 basically made of eight lithofacies units distinguished by their lithology and sedimentary  
336 structures. Each lithofacies is described and interpreted in terms of depositional processes  
337 (Table 1), and most are illustrated on Figure 5.

338 Lithofacies units are often associated together, defining three main facies associations (FA1,  
339 FA2, and FA3), the distribution of which varies depending on the spatial location in the  
340 Guzargues basin and on the vertical position into the Priabonian stratigraphic succession.

341 **FA1** is represented by the alternations of (i) channel-shaped, poorly to weakly sorted  
342 conglomerates (Gu, Gt; Table 1), (ii) matrix-rich, stratified conglomerates (Gm; Table 1), and  
343 (iii) medium- to coarse-grained, cross-bedded sandstones (Sp; Table 1). A general trend in the  
344 vertical evolution of FA1 facies units is recognised through most of the studied sections. In the  
345 lower part of sections, predominant Gu/Gt conglomeratic channels, up to 3m thick and 3 to 5m  
346 wide, contain heterometric, sub-rounded to well-rounded clasts, mainly composed of local  
347 Mesozoic (Upper Jurassic to Lower Cretaceous) carbonates. In some places, they also show  
348 abundant oncoliths (as fragments or complete specimens) probably originated from the  
349 underlying Bartonian formation. In the upper part of sections, conglomeratic bodies in Gm  
350 facies unit are thinner (< 1m) and more laterally continuous (usually more than 10 metres in  
351 width) than in the lower part. In addition to local Mesozoic carbonates, quartz and lydite,  
352 originated from Cévennes and/or Montagne Noire Paleozoic peripheral units, and ginger  
353 (Aptian?) sandstones represent a significant proportion of clasts in channel fillings.

354 **Gu** conglomerates can be interpreted as channel lag (Miall, 1977, 1978; Nemeč and Postma,  
355 1993). The **Gm** and **Gt** facies units present strong similarities with gravel bars in braided  
356 streams (Mack and Leeder, 1999; Miall, 1977; Nemeč and Postma, 1993). **Sp** cross-bedded  
357 sandstones are typical of megaripples deposited by a unidirectional upper to lower flow regime  
358 (Simons et al., 1965; Southard, 1991) produced by subaerial to subaqueous, stream and/or  
359 sheet flows (Hampton and Horton, 2007; Mack and Leeder, 1999). Inferred FA1 depositional  
360 environments are thought to belong to an alluvial fan setting, first supplied by a local catchment  
361 area (lower part of sections), and then by a regional catchment area (upper part of sections).

362



363  
 364 **Fig. 5:** Photographs of outcrops illustrating some typical facies observed in the Priabonian deposits of  
 365 the Guzargues basin. **A:** Facies Gu with carbonate clast alignment underlining tenuous cross-beddings.  
 366 Note scours at the base of the channel (arrows). **B:** Facies Gt showing progressive transition between  
 367 (base) unsorted, highly heterometric massive, stratified conglomerates, and (top) weakly sorted, cross-  
 368 bedded conglomerates. **C:** Alternations between (Sst) cross-stratified sandstones with lenses of  
 369 scattered subrounded gravels and pebbles, and (Gm) matrix-rich, graded, stratified conglomerates with  
 370 weakly sorted pebbles mainly made of Mesozoic carbonates. **D:** Reddish to yellowish laminated silty  
 371 claystones (facies Fm) with intercalation of a decimetric layer of massive fine-grained sandstones (facies  
 372 Sr). **E:** Medium- to coarse-grained cross-bedded sandstones typical of facies Sp. **F:** 50cm-thick  
 373 carbonated horizon showing well-preserved, vertical root casts, probably derived from vegetalization on  
 374 top of massive fine-grained sandstones (Sr).  
 375 Note the occurrence of several pedogenetic carbonate nodules above the irregular top surface of the  
 376 carbonated sandy horizon.

Facies code, Facies name	Lithological features	Sedimentary structures	Inferred depositional processes
<b>Gu.</b> Poorly sorted, massive, channel-shaped conglomerates (Fig. 7A)	Poorly sorted, massive, locally normally graded conglomerates. Highly heterometric, sub-rounded to well-rounded clasts (pebbles to small boulders), mainly composed of local Mesozoic carbonates	Well-defined basal erosional surfaces with gutter/scour structures. Channels displaying few clast imbrications, 50cm up to 3 meters in depth, 3 to 5 meters in width	Channel-lag deposits under subaerial flashy braided-stream flows (Barrier et al., 2010)
<b>Gt.</b> Weakly sorted, cross-bedded, stratified conglomerates with coarse-grained sand lenses (Fig. 7B)	Clast-supported, stratified conglomerates. Weakly sorted, heterometric, sub-rounded clasts (granules to small boulders of Mesozoic carbonates). Occurrences of poorly sorted lenses of coarse-grained sand matrix surrounding individual pebbles	Fining upward infill. Trough cross-bedding	Minor channel fills (Miall, 1978). Transverse- or diagonal-bar deposits under subaerial perennial braided-stream flows (Barrier et al., 2010)
<b>Gm.</b> Matrix-rich, normally graded, stratified conglomerates (Fig. 7C)	Matrix-rich, normally graded, stratified conglomerates. Poorly sorted, subangular to sub-rounded clasts (granules to cobbles) made of local Mesozoic carbonates and some siliceous elements	Some beds with horizontal alignment of clasts. Few clast imbrications into horizontal foreset strata. "Gradual" basal surfaces	Longitudinal-bar deposits under subaerial competent and perennial braided-stream flows (Barrier et al., 2010)
<b>Sst.</b> Moderately sorted, medium- to coarse-grained, cross-stratified sandstones with lenses of sub-rounded gravels and pebbles (Fig. 7C)	Moderately sorted, medium- to coarse-grained sandstones. Layers (and lenses) of well-sorted subrounded clasts (granules to pebbles) composed of Mesozoic carbonates, some Lutetian mudstones and common Bartonian oncoliths (as fragments or complete specimens)	Fining-up trend. Cross-stratification with grading foresets. Well-defined internal erosional surfaces	Bar deposits under subaerial sheet flows or stream flows
<b>Sp.</b> Medium- to coarse-grained, cross-bedded sandstones (Fig. 7E)	Weakly sorted, medium- to coarse-grained sandstones which can contain scattered granules at the base	Cross-stratification. Internal erosional surfaces. Few small scour structures	Megaripple deposits under subaerial sheet flows or stream flows
<b>Sr.</b> Massive, pedoturbated, well-sorted, fine-grained sandstones (Fig. 7D)	Massive, well-sorted, fine-grained sandstones	Pedoturbation (root sleeves, destruction of primary sedimentary structures by root growth). Locally few asymmetrical ripples at the top	Ripple deposits under subaerial sheet flows or stream flows
<b>Fm.</b> Massive, silty claystones with planar siltstone to fine-grained sandstone layers (Fig. 7D)	Reddish to yellowish (also purplish red in some horizons of plastic texture), massive, silty claystones with few thin (mm to cm) layers of well-sorted siltstones and very fine-grained sandstones	Fining-up grading in siltstone to fine-grained sandstone layers	Deposits from suspension fallout in a floodplain. Overbank or waning flood deposits (siltstones and very fine-grained sandstones)
<b>P.</b> Pedogenic carbonate nodules (Fig. 7F)	Indurated, cm to dm carbonate nodules, often scattered within plastic claystones, sometimes coalescent to form continuous carbonate horizons	Vertical root casts	Soil (Miall, 1978) or temporary vegetalized surface

377

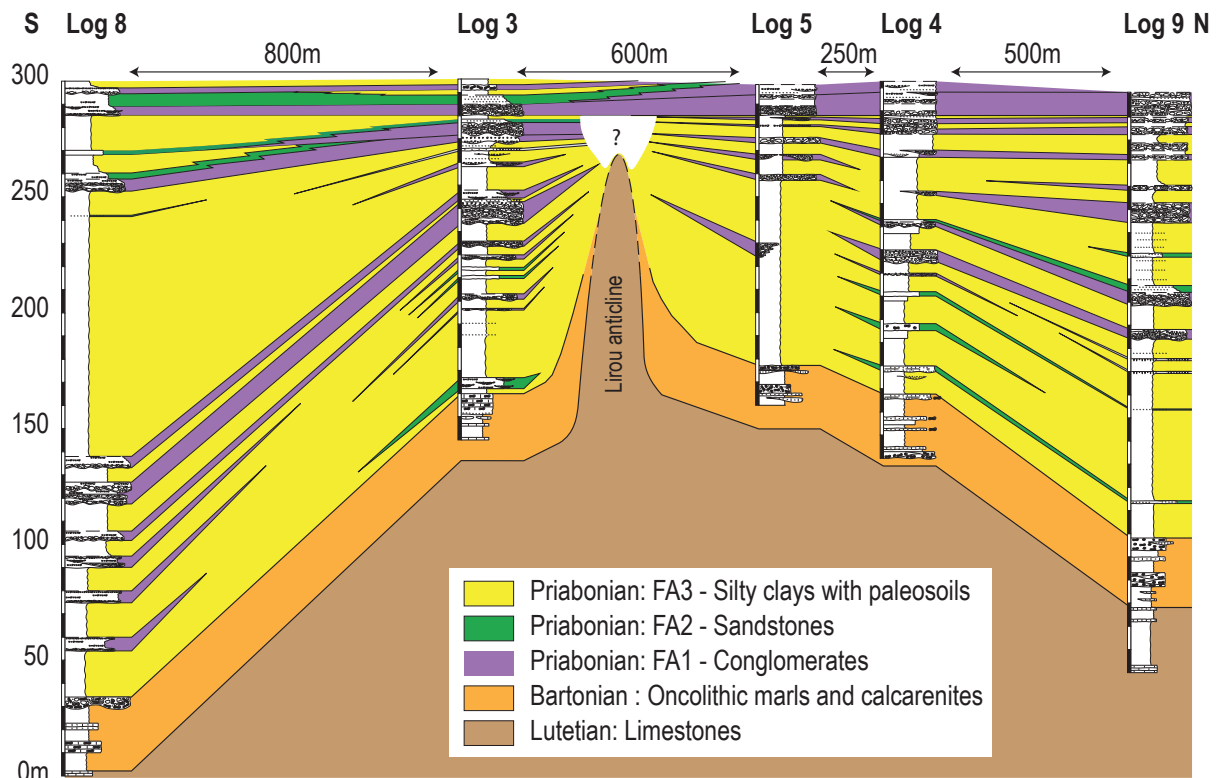
378 **Table 1:** Summary of the main facies features observed in the Priabonian deposits of the Guzargues  
379 basin, and interpretations in terms of depositional processes. Gm, Gt, Sp, Sr, Fm and P, are  
380 abbreviations from the facies code provided by (Miall, 1978). Gu and Sst are abbreviations defined by  
381 (Barrier et al., 2010).

382

383 **FA2** corresponds to the alternation between (i) moderately sorted, medium- to coarse-grained  
384 sandstones with sub-rounded clast lenses (**Sst**; Table 1), and (ii) medium- to coarse-grained  
385 cross-bedded sandstones (**Sp**; Table 1). If local (Mesozoic but also Lutetian) calcareous  
386 elements still represent an important proportion of clasts (granules, gravels, pebbles), siliceous  
387 component (quartz and lydite gravels) is more abundant than in FA1. FA2 depositional  
388 processes are dominated by tractional transport under a unidirectional upper flow regime, with  
389 episodic sheet flows. Inferred depositional environments correspond to the proximal part of a  
390 subaqueous alluvial fan to fan delta, with sediment supplied from both local and regional  
391 catchment areas.

392 **FA3** is mainly represented by yellowish, greenish or reddish silty clays, with plastic texture at  
393 some places, in which are interbedded thin layers of well-sorted siltstones and fine-grained  
394 sandstones (**Fm**; Table 1). Carbonate pedogenic nodules locally form scarce, up to 1m thick,  
395 distinctive layers (**P**; Table 1). Interbedded massive fine-grained sandstones (**Sr**; Table 1)  
396 usually show vertical root traces and more rarely asymmetrical ripple cross-laminations several  
397 centimetres thick at the top.

398 FA3 deposition must be the result of vertical settling from detrital suspensions in standing water  
 399 (Horton and Schmitt, 1996; Miall, 1977). Fine-grained sandstones showing asymmetrical  
 400 ripples and interbedded silty and sandy layers suggest episodic flow regime, related to sheet  
 401 flood events. The occurrence of carbonate nodules records occasional pedogenic processes  
 402 and temporary aerial exposure. Assuming these depositional processes, FA3 should have  
 403 been deposited in the distal part of a subaqueous to subaerial alluvial fan, or in a floodplain  
 404 laterally to major braided distributaries.



405  
 406 **Fig. 6:** Detailed stratigraphic correlation of Priabonian deposits along a 2km-long N-S transect at the  
 407 southeastern border of the Guzargues basin, showing differential subsidence and onlap geometries  
 408 induced by the syndepositional growth of the Lirou anticline. See Fig. 7 for location of logs. Horizontal  
 409 correlation lines set at the maximum of progradation recorded by several meters-thick, stacked  
 410 conglomeratic channels that closely rests on Lutetian limestones at the apex of the Lirou anticline.

411  
 412 The 10 studied sections show vertical variations in the FA succession (basically FA1-FA2 or  
 413 FA2-FA3 alternations) forming elementary sequences between several metres and tens of  
 414 metres thick (Fig. 6). As indicated by the various inferred depositional environments for FA,  
 415 these elementary sequences, made up of alternatively proximal and distal deposits, are  
 416 arranged into overall trends measuring several tens of metres thick, recording progradational  
 417 and retrogradational evolutions.

418 At the scale of the Guzargues basin, the large FA alternations are describing a whole  
 419 progradational, then retrogradational, and finally progradational evolution, which is easily



420 recognised on the field. These trends were used to correlate Priabonian deposits at basin scale  
421 and, combined with aerial photograph interpretation, to produce a detailed geological map that  
422 allows building cross-sections.

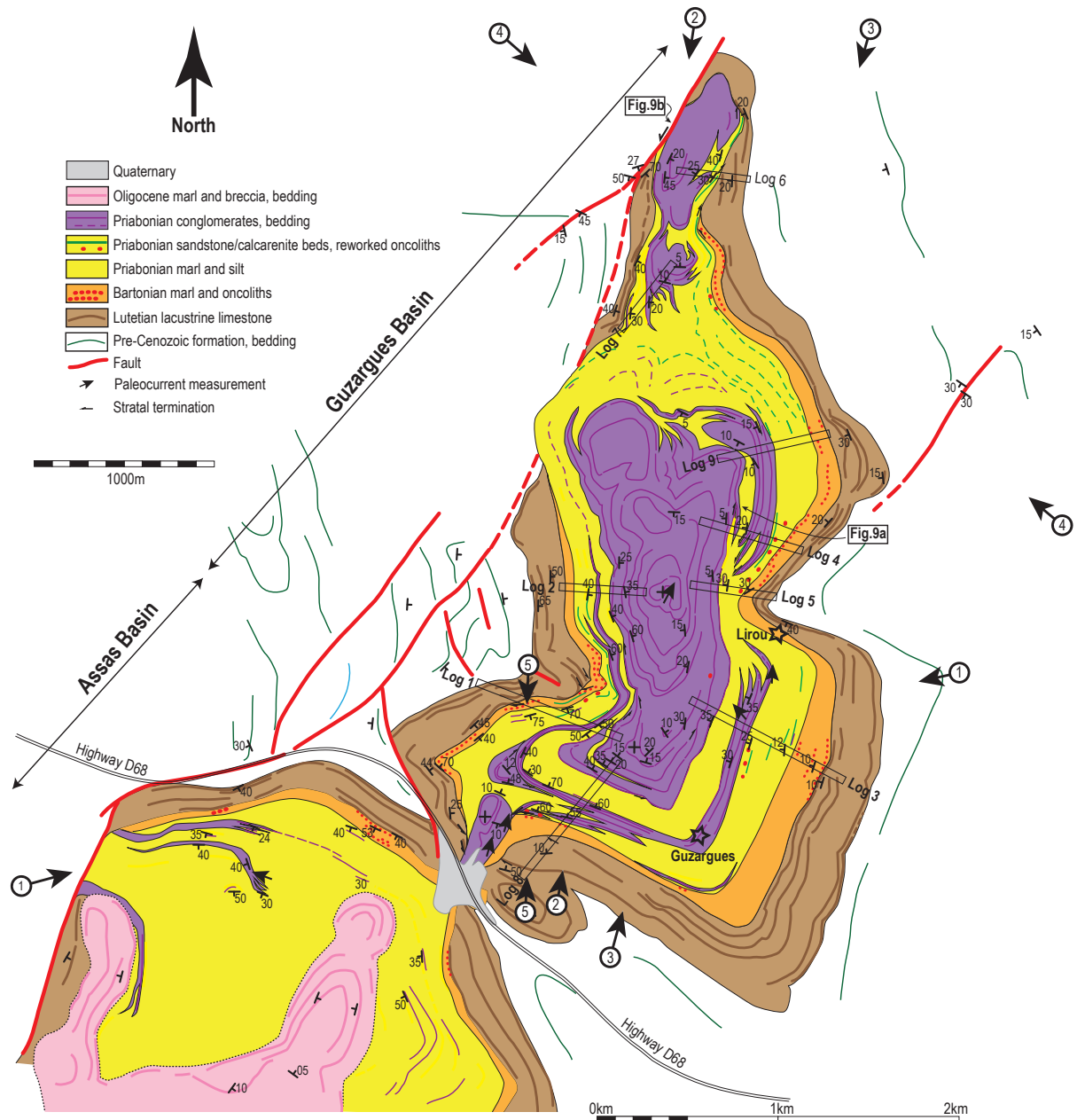
423

#### 424 **4-3. Tectonic-sedimentation relationships in the Guzargues basin**

425

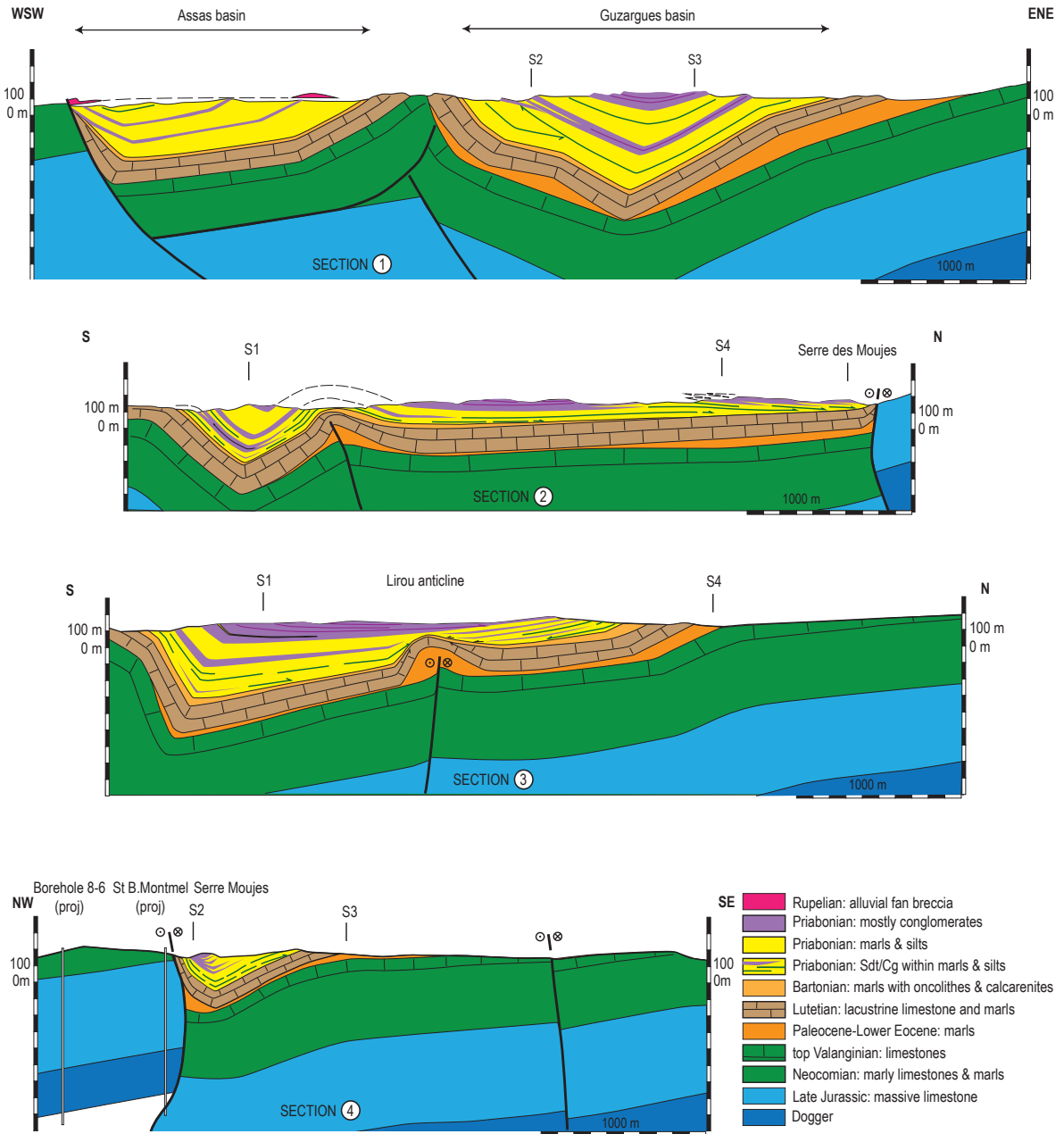
426 The detailed geological map (Fig.7) and cross-sections (Fig. 8) of Guzargues basin show  
427 sequences of Priabonian conglomerates interfingering with marls, that are involved in gentle  
428 folding of complex geometry. To the south, the basin is separated from the contemporaneous  
429 Assas Basin by a NW-SE anticline, cored by Valanginian (Fig.7 and Fig.8 - Section 1). North-  
430 south sections of Guzargues basin (Fig.8 - Sections 2, 3) display an asymmetrical syncline  
431 structure: the southern limb is steeply dipping north, whereas the northern limb extends over  
432 3 to 4 km in a gently dipping or subhorizontal position. In addition, the basal part of the  
433 Priabonian is affected by ENE-trending anticlines, while the youngest conglomeratic  
434 Priabonian seals the anticline (Fig. 8 - Section 3).

435 *The Lirou anticline* - The Bartonian and the base of the Priabonian sequence (isolated  
436 sandstone and conglomerate beds in marls) are wedging towards an anticline with an EW-  
437 oriented, W-plunging axis. Conglomerate beds isolated in the silt and marls are observed on-  
438 lapping both flanks of the anticline (Fig.6), and they display diverging bedding away from the  
439 anticline (Fig. 7, Fig. 9a). The upper conglomeratic interval, corresponding to the final  
440 progradational trend recorded by Priabonian deposits, progrades northwards across the whole  
441 basin, over a silt and shale interval and seals the Lirou anticline (Fig. 6). Folding affects the  
442 Lutetian lacustrine limestones, and the top of the Lutetian is eroded in the crest of the anticline.  
443 Variable thickness of Latest Cretaceous to Early Eocene marls suggests a decollement with  
444 the underlying monocline Valanginian limestones. The latter is affected by a sub-vertical, NE-  
445 trending fault, which displays a left-lateral component of movement (Fig. 8 - Section 3). These  
446 observations lead to the following points: i) folding was initiated during Pyrenean shortening,  
447 and was still active during deposition of the early Priabonian; ii) folding of the Paleogene  
448 sequences is detached above the Valanginian limestone, through a detachment within the Late  
449 Cretaceous-Early Eocene marls; iii) folding is related with a NE-trending left lateral strike-slip.



450  
 451 **Fig. 7:** Detailed geological and structural map of the Guzargues basin (north of Highway D68, while  
 452 Assas sub-basin is located south of the highway). Location of the sedimentological logs 1 to 9 reported  
 453 on Fig. 6 are indicated by fine black rectangles. Position of the structural cross-sections extremities (Fig.  
 454 8 and 9) are given by black arrows.

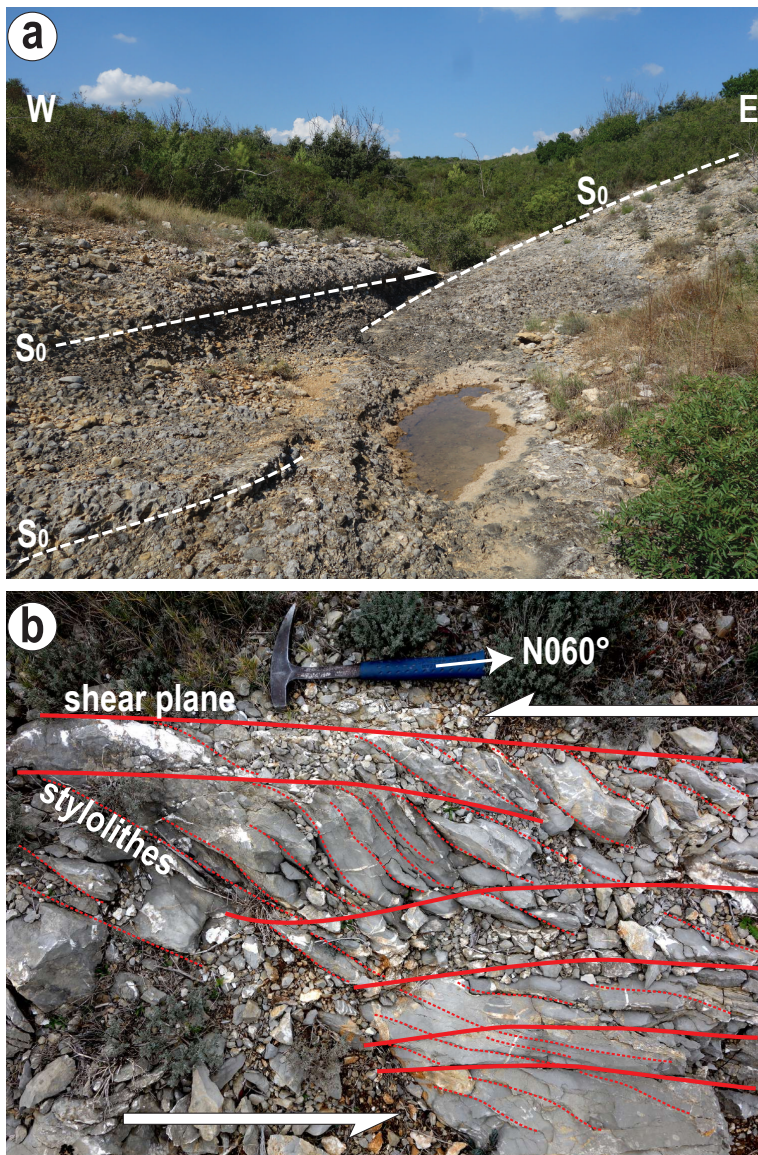
455



456

457 **Fig. 8:** Structural sections across the Guzargues basin; see location on Fig. 7.





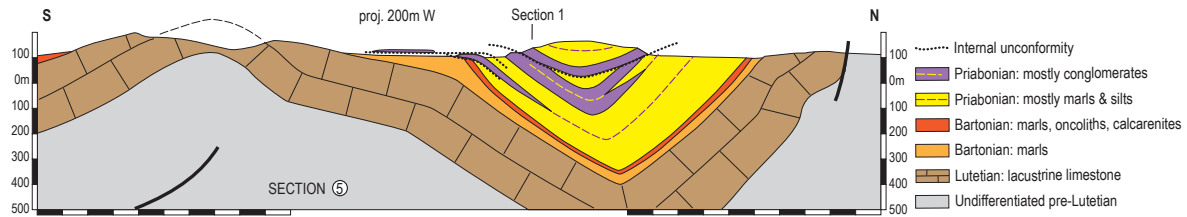
458

459 **Fig. 9:** **a:** internal onlap within the Priabonian conglomerates, which illustrates syndepositional folding  
 460 of the Lirou anticline. Location on map Fig. 7. **b:** Penetrative deformation of the Jurassic limestones  
 461 along the basin-bounding fault, indicating left-lateral kinematics. Serre de Moujes, location on maps Fig.  
 462 7.

463

464 *The southeastern boundary* – Figure 10 shows up to three stacked, angular unconformities,  
 465 which affect the lower Priabonian sequences along the southern flank of an EW syn-  
 466 sedimentary syncline. These angular unconformities pass northwards to correlative  
 467 conformities, while they converge southwards, towards the basin boundary, corresponding to  
 468 an E-trending anticline of Lutetian limestone. This anticline is locally eroded by a present-day  
 469 transverse valley, but mapping reveals that sub-horizontal Priabonian conglomerates are  
 470 exposed within this valley and that they laterally onlap onto the incised carbonates (Fig. 7).  
 471 Clasts imbrication within the fluvial conglomerates indicates a consistent northwards

472 paleocurrent in the paleo-valley. Very thin (several tens of metres) in the transverse valley, the  
 473 Priabonian formations thicken rapidly northward within 1 kilometre distance, from less than  
 474 300 m to 450 m, and it exceeds 600 m in the syncline axis. In addition, fluvial conglomerate  
 475 belts pass laterally and distally (northwards) to silts and marls of alluvial plain facies. These  
 476 observations clearly show that: i) the syncline was formed during deposition of the Priabonian ;  
 477 ii) the basin was fed by a north-flowing paleoriver, incised into the growing Lutetian limestone  
 478 E-W anticline.



479  
 480 **Fig. 10:** Detailed structural section in the south of Guzargues basin showing growth syncline and internal  
 481 angular unconformities. See location of Section 5 on Fig. 7.

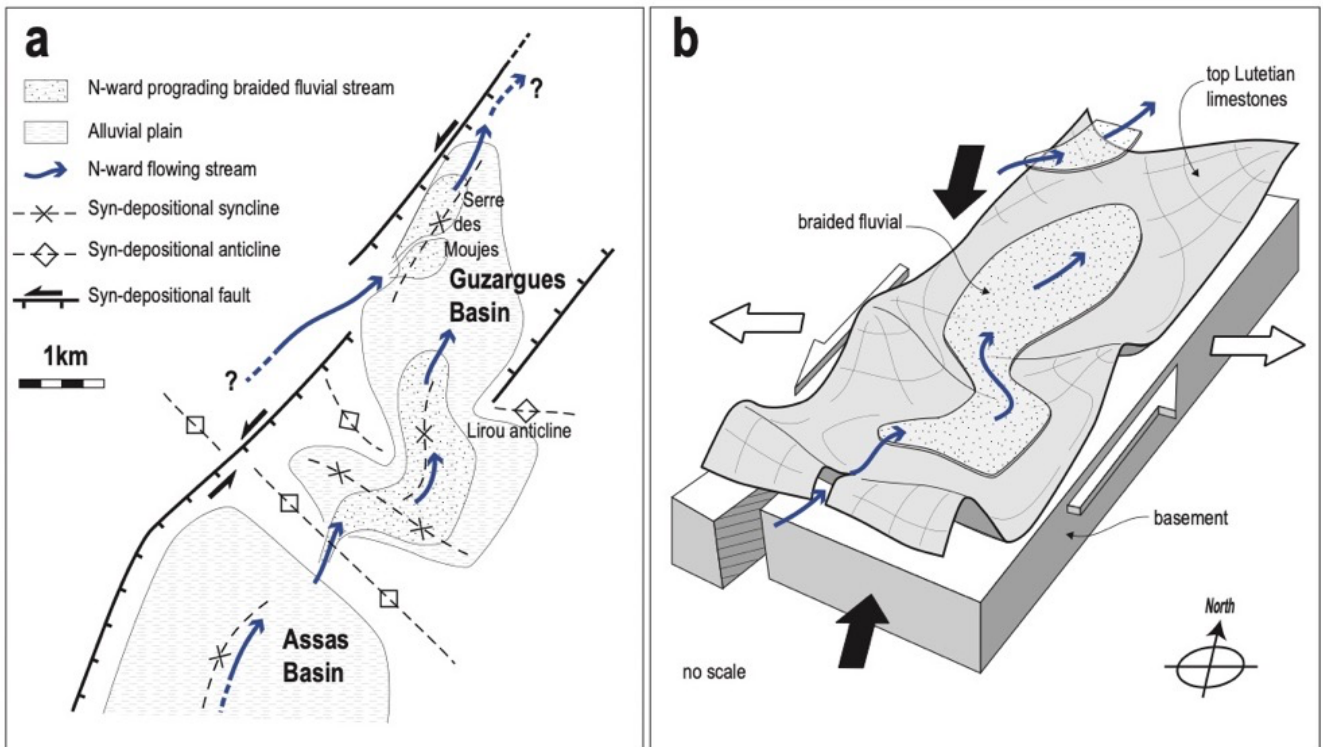
482  
 483 *Serre de Moujes* - The northern part of the basin corresponds to a syncline trending N020°,  
 484 that involves Lutetian limestones and Priabonian conglomerates (Fig. 7). The conglomerates  
 485 are more developed on the steep western flank, where they unconformably rest over the  
 486 steeply dipping Lutetian limestones, and they grade eastwards to distal silts and marls (Fig. 8  
 487 - Section 4). Along the eastern flank of the syncline, Priabonian formations are onlapping onto  
 488 the Lutetian limestone; in addition, the Bartonian oncolith formation is transgressed towards  
 489 the north by the Priabonian. Onlapping surfaces point to a pre-existing synform of Lutetian  
 490 limestones prior to Priabonian deposition. The conglomerate belt is separated from that of the  
 491 main part of the basin, suggesting the presence of a smaller, northern, sub-basin with a distinct  
 492 feeder that supplies clastic sediments across the western boundary (Fig.8 – Section 2).  
 493 Unfortunately, no clear evidence of paleocurrent were found. North-south correlations across  
 494 the entire Guzargues basins shows that the northern sub-basin represents the youngest  
 495 depocentre of the whole basin (Fig. 8 - Section 1). To the NW, Priabonian is directly in contact  
 496 with the Mesozoic carbonates through a sub-vertical faulted boundary. In the *Serre de Moujes*,  
 497 outcrop in the damage zone of the bordering fault reveals sets of associated fractures and  
 498 dissolution surfaces, consistent with a left-lateral strike-slip motion (Fig. 9b). Unfortunately, no  
 499 slickensides could be observed to constrain the respective vertical and horizontal components  
 500 of slip. Saint-Bauzille-de-Montmel borehole (located 1.5 km north, along strike) constrains a  
 501 curved geometry for this fault and provides evidence for a 700m vertical offset (Fig. 8 - Section  
 502 4). Considering the fault geometry and the kinematic observations on the outcrop, a dominantly  
 503 strike-slip movement along this bordering fault is suggested during Priabonian and the  
 504 important vertical offset implies several kilometres of cumulated lateral offset. A significant part

505 of such offset may be inherited from earlier (Pyrenean) tectonic phases. These observations  
 506 argue for i) deposition of Priabonian syn-tectonic sediments in a hanging-wall syncline,  
 507 controlled by the activity of the N020°-trending bounding fault, and ii) accommodation of a  
 508 significant amount a left-lateral strike-slip, by this inherited fault.

509

#### 510 **4-4. Tectonics - paleoenvironment relationships in the Guzargues basin**

511



512  
 513 **Fig. 11: a:** Sketch map of the paleoenvironments in the Guzargues basin, in relation with the Priabonian  
 514 tectonics. **b:** Conceptual tridimensional representation (no scale intended) of the interaction between  
 515 Priabonian kinematics and sedimentation in the Guzargues basin. Braided fluvial conglomerates  
 516 accumulate in the most subsiding parts, i.e. the actively deforming synclines that affect the Mesozoic-  
 517 Lutetian cover, detached over the basement. See text for explanations.

518

519 Figure 11a provides a synthetic view of the paleoenvironment distribution across the  
 520 Guzargues Basin during Priabonian. Fluvial sediments were delivered through an incised  
 521 canyon across a growing anticline, which separates Assas (to the south) and Guzargues  
 522 basins. The belt of northward-flowing fluvial channels preferably occupied the most subsiding  
 523 parts of the basin: i) in the south, parallel to the bordering growing anticline and, ii) in the overall  
 524 N-trending axis of the syn-depositional syncline. The latter was controlled by a set of NNE-  
 525 trending faults which display map- and outcrop-scale evidences of normal faulting and left-  
 526 lateral strike-slip. The secondary fluvial conglomerates depocenter of Serre de Moujes, in the  
 527 northern part of the basin, witnesses an additional fluvial input to the basin, across a relay or



528 a jog in the bordering fault system. The syn-depositional Priabonian sequence is therefore  
529 controlled by folding of the Mesozoic through the Lutetian cover detached over the Triassic  
530 decollement, corresponding to an overall transcurrent, left-lateral kinematics, along the NNE-  
531 trending faults (Fig. 11b). The kinematics documented in the Guzargues basin result from NS  
532 shortening combined with EW extension,

533

## 534 **5. Les-Matelles and Saint-Martin-de-Londres Priabonian basins**

535

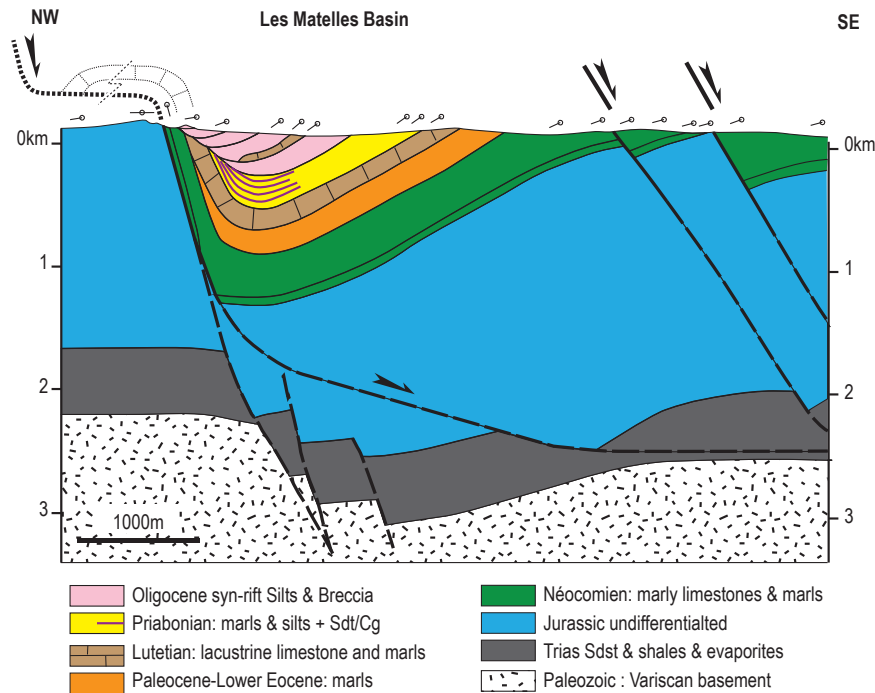
### 536 **5-1. Les-Matelles basin**

537

538 The overall geometry of Les-Matelles basin (LMB) is that of an Oligocene syn-rift hanging-wall  
539 syncline, controlled by a NNE-trending normal fault (Fig. 2), known as the Matelles-Corconne  
540 Fault (Benedicto et al., 1999). The Priabonian sequence mostly consists of marls and  
541 siltstones with rare conglomerate beds. Paleocurrent measurements in the channelised fluvial  
542 conglomerates indicate northwest to northeast flowing channels (Egerton, 1996). Detailed  
543 mapping (Benedicto, 1996) revealed that the underlying Priabonian sequence also presents  
544 growth structures in an asymmetric syncline, that displays a NW limb steeper ( $\geq 40^\circ$ ) and  
545 thinner than the SE limb (Fig. 12). Sequential tectonic restoration of transverse sections  
546 indicates an extensional offset across Les-Matelles-Corconne Fault of some 375 m, during  
547 Priabonian (Benedicto et al., 1999).

548 In the southernmost part of the basin, Priabonian unconformably overlies the syn-orogenic  
549 breccia of Paleocene age, related to the activity of the Montpellier thrust (Andrieux et al., 1971).

550 In the central segment of the basin, Priabonian is conformable over the distal syn-orogenic  
551 marls and oncoliths of Bartonian age. Finally, in the northern extension of this basin, Priabonian  
552 is unconformable over Neocomian marly limestones, which are deformed by EW-trending  
553 compressional structures. Such folds and thrusts are correlated to the Pic-Saint-Loup thrust,  
554 active during Bartonian (Philip et al., 1978). Considered at the scale of the basin, the  
555 Priabonian is thus unconformable over pre-Pyrenean deformed series, as well as syn-orogenic  
556 Pyrenean sedimentation. Finally, the syn-rift Late Rupelian breccia are unconformably  
557 overlying the Priabonian (Crochet, 1984).



558

559 **Fig. 12:** Structural section across Les-Matelles basin (from surface data and seismic profile) showing  
 560 syn-extension deposition of Priabonian units. Modified after (Benedicto et al., 1999).

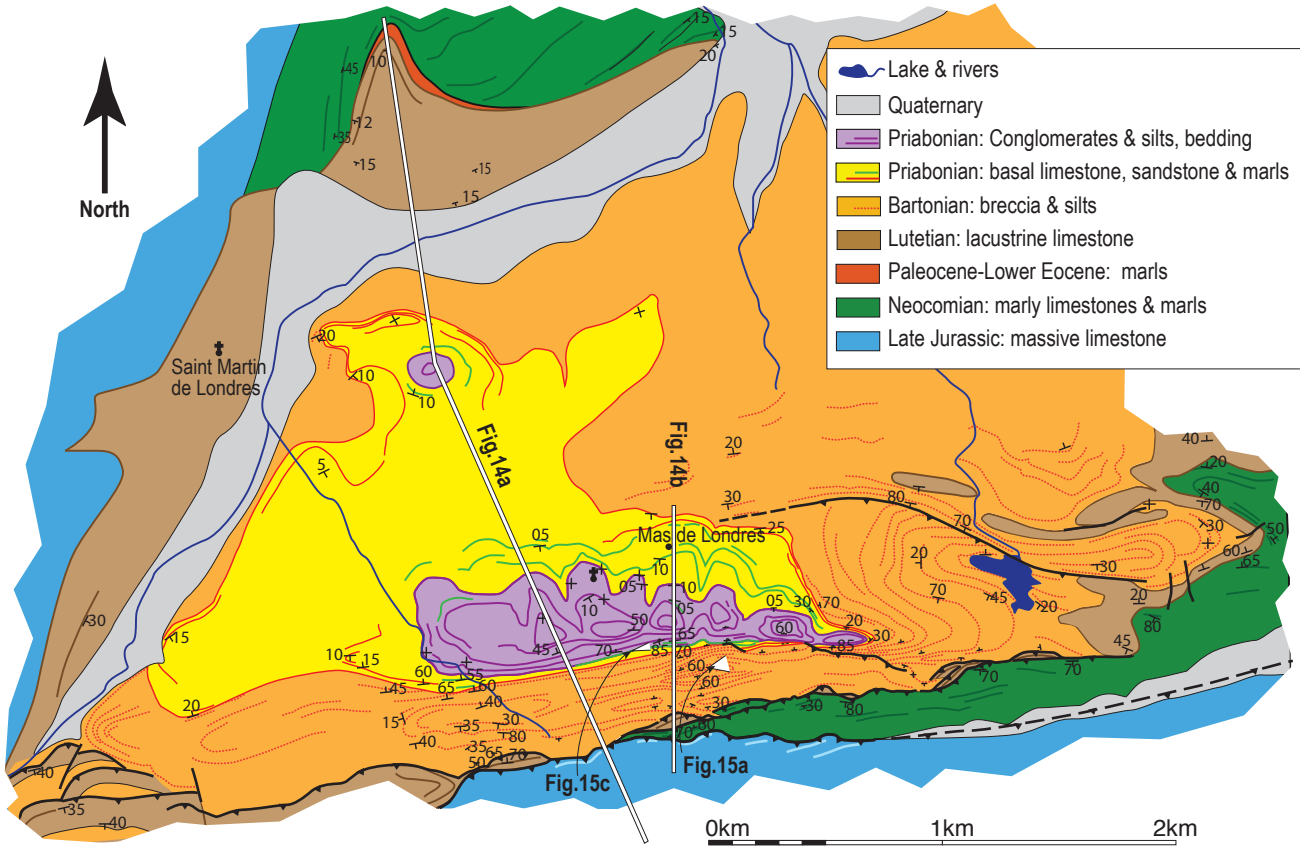
561

## 562 5-2. Saint-Martin-de-Londres basin

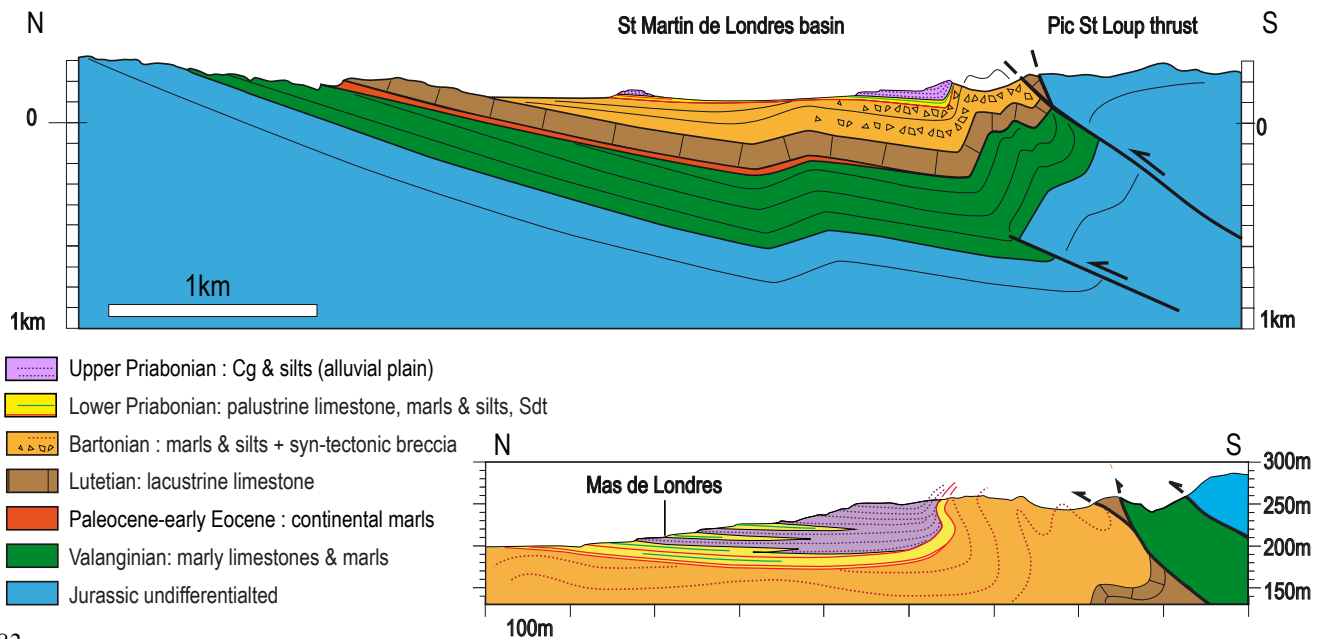
563

564 Saint-Martin-de-Londres basin (SMLB) extends in an EW asymmetric syncline, immediately  
 565 north of the Pic-Saint-Loup thrust, a structure of the Pyrenean fold and thrust belt (Fig. 2).  
 566 Above an unconformity over the Neocomian, the basin sequence starts with continental marls  
 567 and thin beds of lacustrine limestones of latest Cretaceous to Paleocene age (Crochet, 1984;  
 568 Freytet, 1971; Philip et al., 1978), which are the distal correlative of the syntectonic  
 569 « Vitrollian » breccia, deposited along the Montpellier thrust.

570 Lutetian lacustrine limestones, transgressive over Late Jurassic to Paleocene formations, form  
 571 an 80 m to 100 m-thick slab that designs a wide, low amplitude, EW-oriented syncline (Fig.  
 572 13). The overlying breccia, dated to the Bartonian (Philip et al., 1978), consists of local, late  
 573 Jurassic, Neocomian and Lutetian limestones, derived from erosion of the active Pic-Saint-  
 574 Loup thrust front. They pass northwards to distal continental marls and silts, which present  
 575 syn-tectonic growth structures. The southern boundary of the basin has been intensely folded  
 576 and faulted in relation with the Pyrenean Pic-Saint-Loup thrust, during Bartonian time (Fig.14).  
 577 The Priabonian sequence unconformably overlies the Bartonian breccia; to the east, it seals  
 578 an intra-Bartonian thrust propagation fold (Fig.13), which requires erosion of the Pyrenean-  
 579 related structure prior to Priabonian deposition.

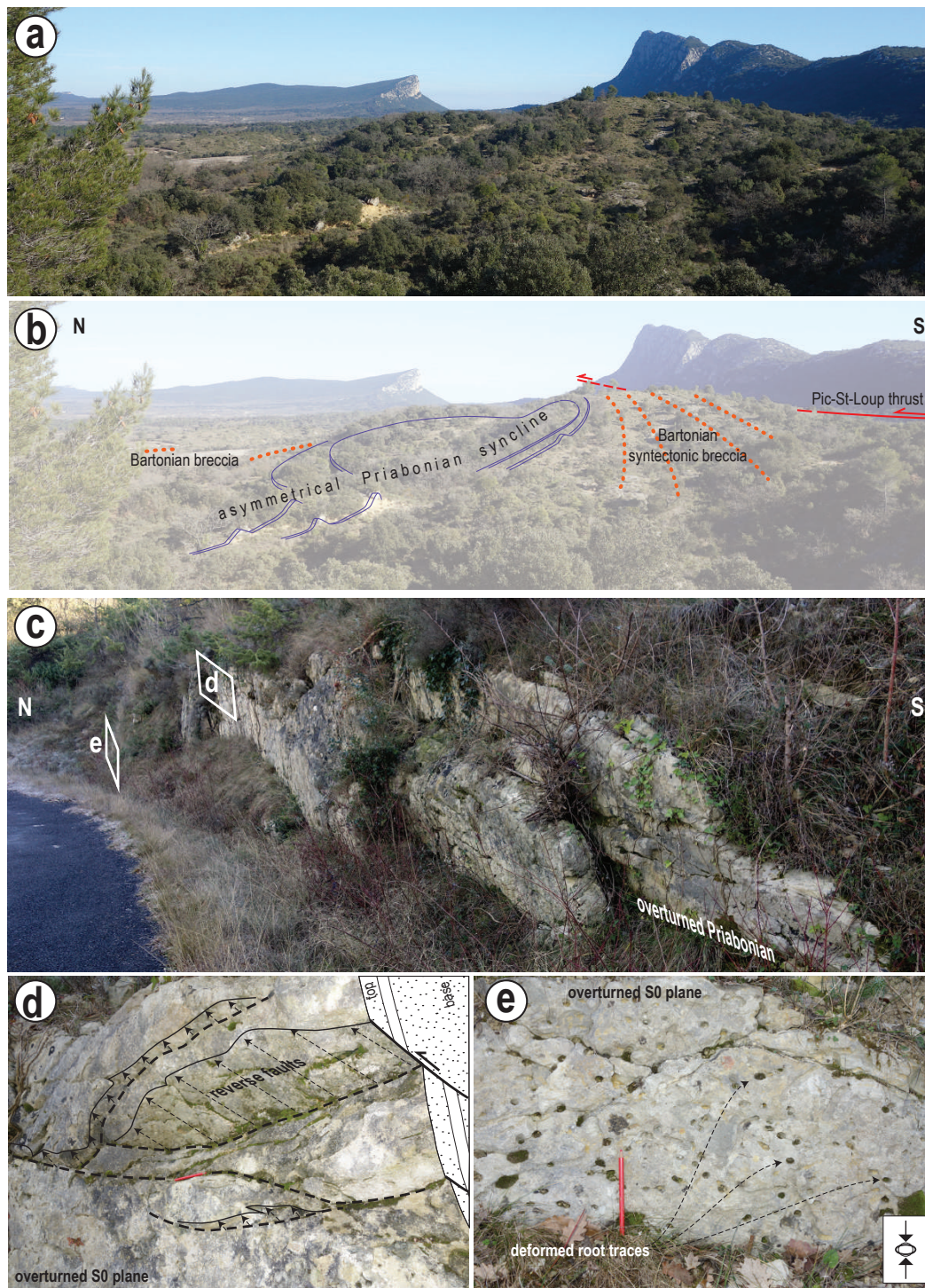


580  
 581 **Fig. 13:** Detailed geological map of Saint-Martin-de-Londres basin. Position of sections Fig. 14 indicated  
 582 as white line. The black dot and cross points to the churches of the villages.



583  
 584 **Fig. 14:** Structural section across St Martin-de-Londres basin: a - general ; b – detailed, showing syn-  
 585 depositional compression during Priabonian.





586

587 **Fig. 15:** **a** and **b:** general view of the eastern end of St-Martin-de-Londres Priabonian basin, an  
 588 asymmetrical growth syncline, unconformable over the synorogenic Bartonian breccia, which were  
 589 generated along the pyrenean Pic-St-Loup thrust. **c:** overturned Priabonian sandstone along the  
 590 southern limb of the asymmetric syncline. **d;** detail of the previous outcrop displaying small scale reverse  
 591 faults that provide evidence for N-S compressive deformation. **E:** deformed root traces, evidence for  
 592 pre-lithification N-S compressive deformation of the Priabonian sandstone bed, prior to its folding.  
 593 Outcrop location on Fig. 13.

594

595 Along the southern margin of the SMLB, the Priabonian sequence designs an asymmetric  
 596 syncline with sub-vertical to overturned southern limb (Fig. 15a,b.). The sequence starts with  
 597 a thin level of finely laminated limestone that contains bioclasts and charophytes characterising  
 598 a lacustrine / palustrine environment. Laterally, the limestone passes to thicker and more  
 599 massive beds of lacustrine mudstone. The thin basal limestone is correlated to the north of the  
 600 basin, with 10 m to 15 m thick marls and carbonates deposited in an arid, evaporitic  
 601 environment. Above the limestones, along the central southern margin only, are found grey  
 602 marls including several thin beds of glauconitic sandstones with bioclasts and rare foraminifera  
 603 (Egerton, 1996). This shallow marine sandstone passes upwards to marls and siltstones  
 604 including thin bioturbated sandstone beds, deposited in a floodplain, similar to those described  
 605 in LMB. In the upright, southern limb of the syncline, these sandstone beds are affected by  
 606 small scale reverse faults (Fig.15c). They also display soft penetrative deformation of initially  
 607 cylindrical root traces (Fig. 15d), which indicate an early, pre-lithification, N-S shortening prior  
 608 to folding. Finally, up to 50 m stacked, channelized conglomerates, are deposited in several-  
 609 metres-thick levels, interbedded with siltstones and marls. The high ratio of channelized  
 610 conglomerates vs floodplain marls and siltstones is more in line with Guzargues than with Les-  
 611 Matelles basins. Conglomerates are clast-supported and rather well-sorted. Clasts are  
 612 polygenic, including significant number of quartz veins and black cherts, derived from the  
 613 Paleozoic deformed basement. Distinctive clasts of glauconitic sandstones and calcarenites  
 614 containing Albian orbitolines cannot be related to any local source, as the Mesozoic sequence  
 615 is interrupted above the Valanginian due to the regional erosion of the Durancian Isthmus  
 616 (Husson, 2013). Such clasts, also been identified in Les-Matelles and Montferrier Priabonian  
 617 outcrops are imbricated under the influences of north to northwestwards paleocurrents  
 618 (Egerton, 1996), and thus correspond to a southerly derived material (Freytet, 1971).  
 619 The Priabonian sequence of SMLB unconformable over Pyrenean structures, and containing  
 620 clasts supplied by a southerly derived sedimentation was deposited in a N-S compressional  
 621 setting, related to reactivation of the Pyrenean Pic-Saint-Loup Thrust.

622

## 623 **6. Seismic sequence analysis of the Hérault Basin**

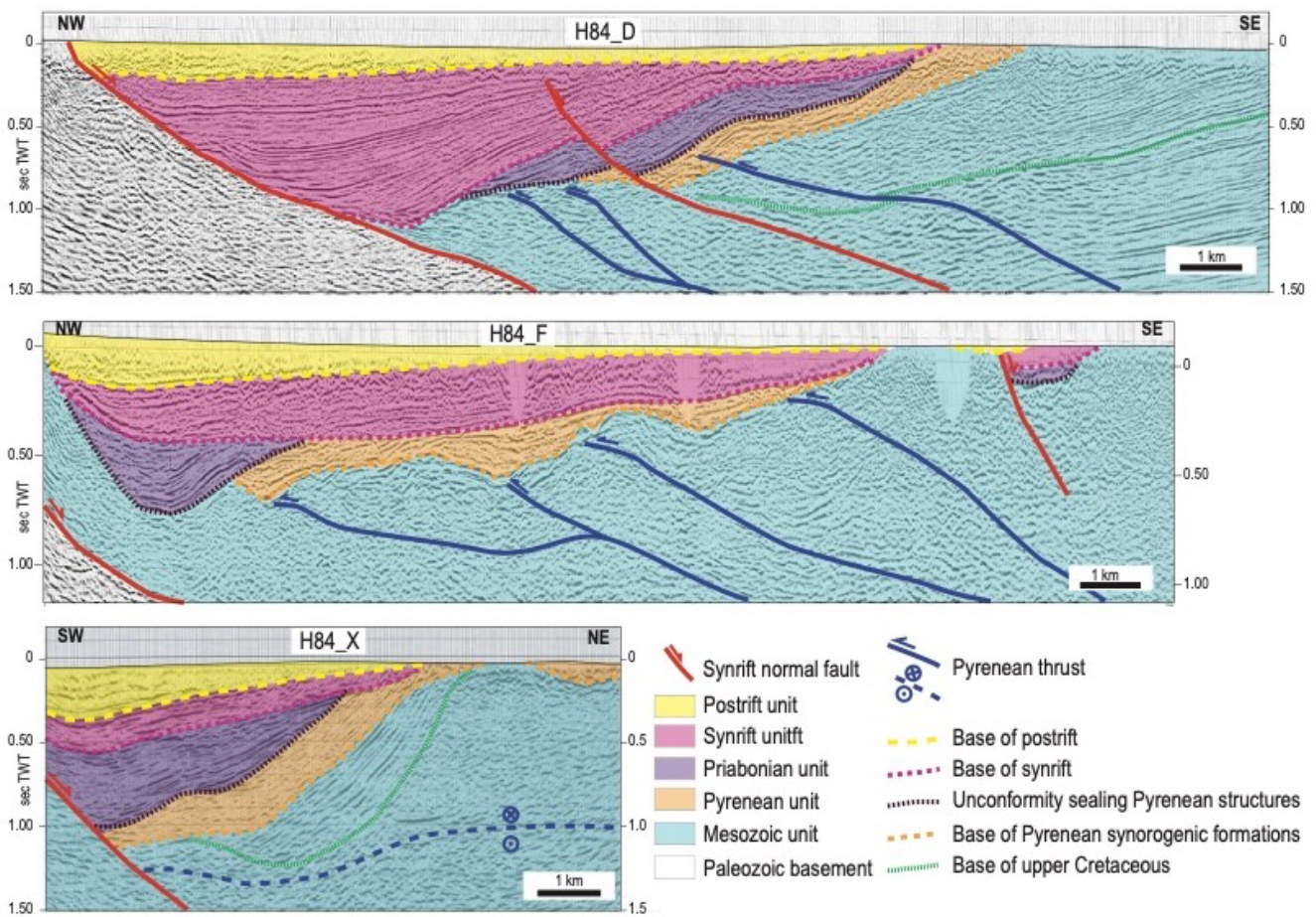
624

625 The Hérault Basin (HB) is a NNE-SSW asymmetric half-graben developed along the Cévennes  
 626 Fault, formed in relation with the rifting of the Gulf of Lion (Arthaud et al., 1981; Maerten and  
 627 Séranne, 1995; Séranne, 1999). It covers the western part of the Pyrenean Montpellier thrust  
 628 (Fig. 2) and is filled by up to 1500m-thick succession of rift and post-rift sequences. The syn-  
 629 rift and earlier Pyrenean structures are therefore mostly covered, which lead us to investigate  
 630 the Pyrenean to syn-rift transition through subsurface data.

631 The basin sequence consists of (i) Rupelian to Aquitanian, continental and lacustrine

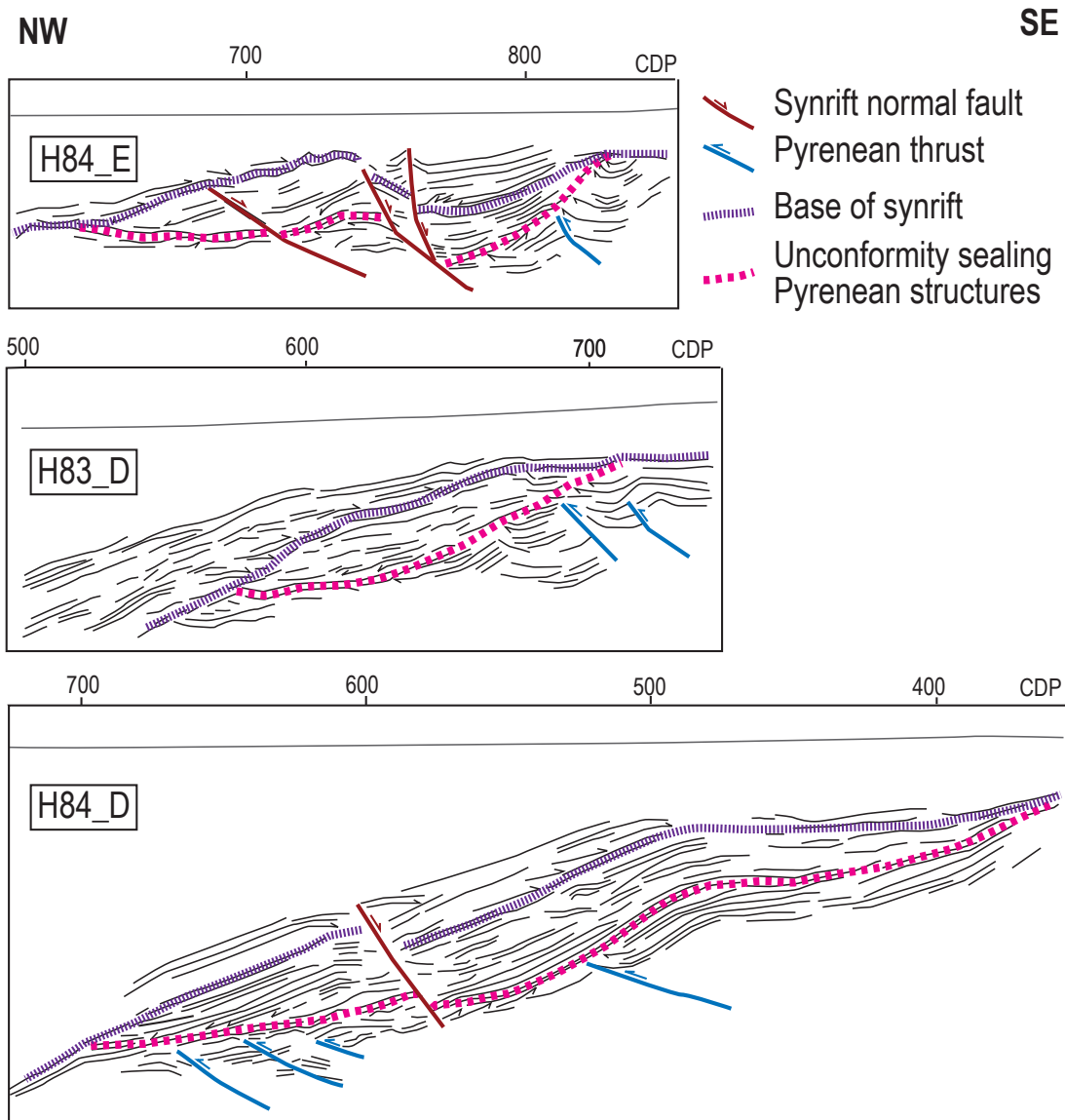


632 formations, and (ii) Burdigalian to Langhian, marine to fluvial post-rift deposits, forming syn-rift  
 633 and post-rift sequences separated by a major unconformity. The pre-rift substratum consists  
 634 of Permian to Jurassic sequence, as well as mid-Cretaceous bauxite deposits, which have  
 635 been sampled by several boreholes (Berger et al., 1981; Lajoinie and Laville, 1979). In  
 636 addition, syn-tectonic Pyrenean Paleocene to Eocene formations (poorly exposed along the  
 637 eastern margin of the basin) and Mesozoic carbonates deformed during Pyrenean  
 638 compression can be extrapolated beneath the basin, and several Pyrenean thrusts repeating  
 639 parts of the Jurassic sequence are documented (Alabouvette et al., 1982; Berger et al., 1981).



641 **Fig. 16:** Seismic profiles representative of the Hérault basin (H84D, H84F, H84X). The purple sequence  
 642 interpreted as Priabonian (see discussion in text) is intermediate between the Pyrenean synorogenic  
 643 units and the Oligocene syn-rift sequence. See location on Fig. 2 and 18.

644  
 645 Two geophysical surveys acquired in 1983 and 1984, then reprocessed in 2005-2008 (Serrano  
 646 and Hanot, 2005), provide a regular seismic coverage (Fig. 2) of sufficient quality to examine  
 647 the seismic units underlying the syn-rift sequence (Fig. 16). Some of these seismic sections  
 648 were already interpreted by (Maerten and Séranne, 1995) who focused their study on the  
 649 geometry of syn- and post-rift units.



650

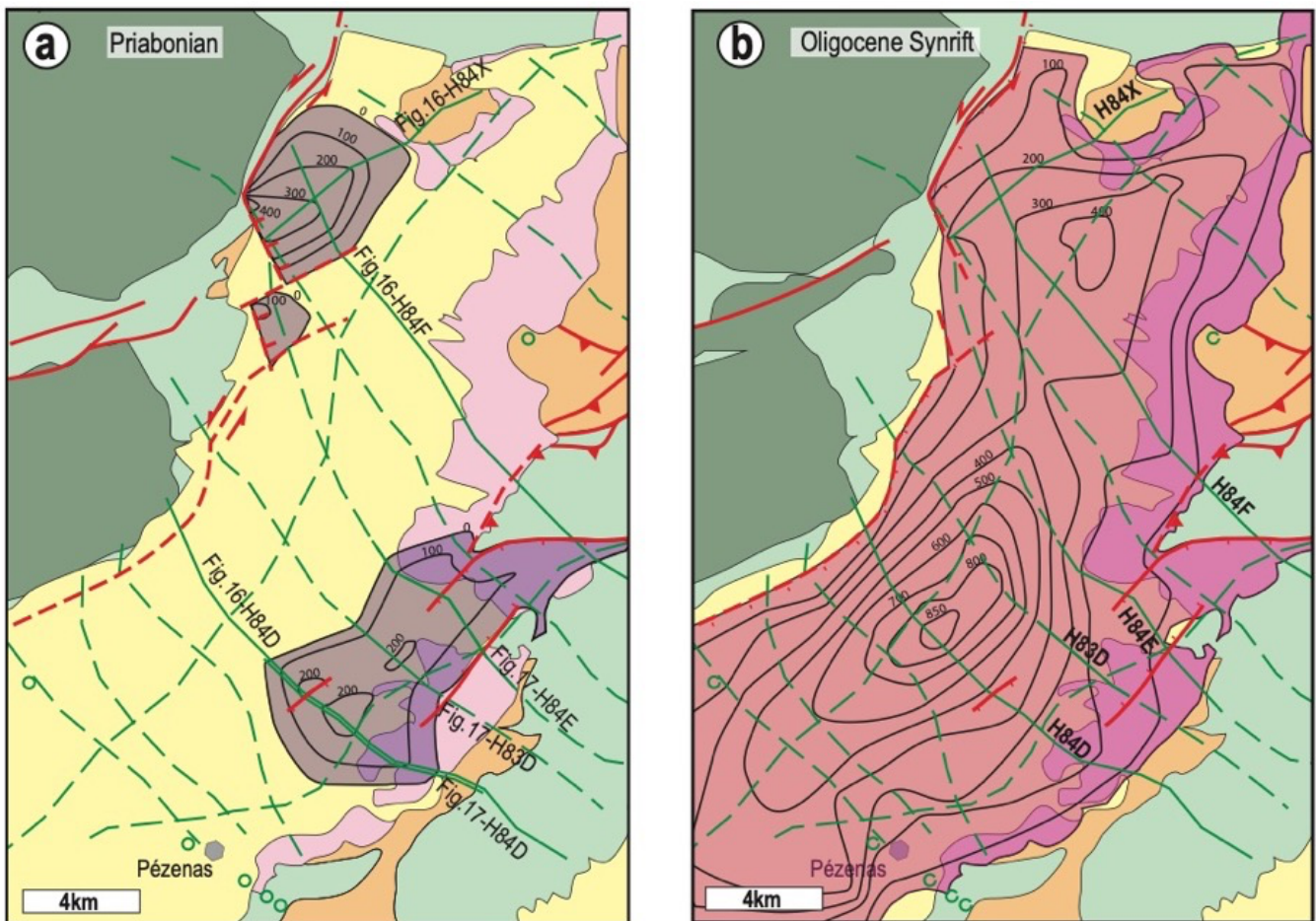
651 **Fig. 17:** Line drawings of parts of selected seismic profiles in the Hérault basin showing the lower and  
 652 upper erosional boundaries of the intermediate sequence. See location on Fig.18.

653

654 Reinterpretation of the seismic profiles allows us to identify, in several parts of the basin, a  
 655 distinctive seismic unit below the syn-rift deposits (Fig.16). It is bounded by angular  
 656 unconformities both at the top and at the base and displays significant thickness variations and  
 657 complex internal geometries. Geometrical relationships with underlying and overlying seismic  
 658 sequences define its relative stratigraphy: (i) It is truncated by typical syn-rift sequences and  
 659 is affected by the extensional syn-rift faults; (ii) It unconformably rests on pre-rift units affected  
 660 by Pyrenean reverse faults (Fig. 17). This intermediate seismic unit, undrilled by any  
 661 boreholes, does not correlate with surface exposures. However, comparison with field  
 662 observations in the GB, SMLB and LMB point out a similar structural and stratigraphic position  
 663 suggestive of a Priabonian age. Mapping of this intermediate interval, of proposed Priabonian



664 age, across the Hérault basin shows a discontinuous sequence including two main  
 665 depocentres (Fig. 18 a). One depocentre is located where the Cévennes Fault displays a  
 666 significant change from an overall NE-SE direction to a SSE-trending orientation. H84X profile  
 667 (Fig.16) shows evidence for Priabonian syn-depositional, dip-slip movement across the SSE-  
 668 trending fault segment. Such a geometry suggests a left-lateral movement along the Cévennes  
 669 fault, associated with a dip-slip across the SSE segment which represents a releasing bend  
 670 (e.g. (Christie-Blick and Biddle, 1985; Cunningham and Mann, 2007) of the master fault. A  
 671 second depocentre is located along the SE margin of the Hérault basin, controlled by NE-  
 672 trending faults that offset the earlier Pyrenean Montpellier thrust.



674 **Fig. 18:** Isopach maps of Priabonian (a) and of syn-rift (b) sequences in the Hérault basin, superimposed  
 675 onto a simplified geological map (same legend as in Fig. 2, and location in Fig. 2). Contouring of  
 676 depocenters in metres. The seismic profiles used in the study are represented in stippled green lines;  
 677 plain green lines with labels correspond to the profiles shown in Fig. 16 and 17. Faults are represented  
 678 in red.

679  
 680 Isobaths of the base syn-rift (Fig. 18 b) depict the depocentre of the syn- and post-rift Oligo-  
 681 Miocene basin. Comparing the two maps (Fig. 18 a and b) clearly shows that the successive  
 682 sequences were controlled by two distinct tectonics settings and kinematics. The distribution

683 and NE-SW overall orientation of the Oligo-Miocene depocentre, and the presence of a  
 684 transfer zone (roughly parallel to H83E profile) are consistent with NW-SE extension across  
 685 the Cévennes-fault (Maerten and Séranne, 1995). Our data do not support such a transfer  
 686 zone active during the Priabonian.

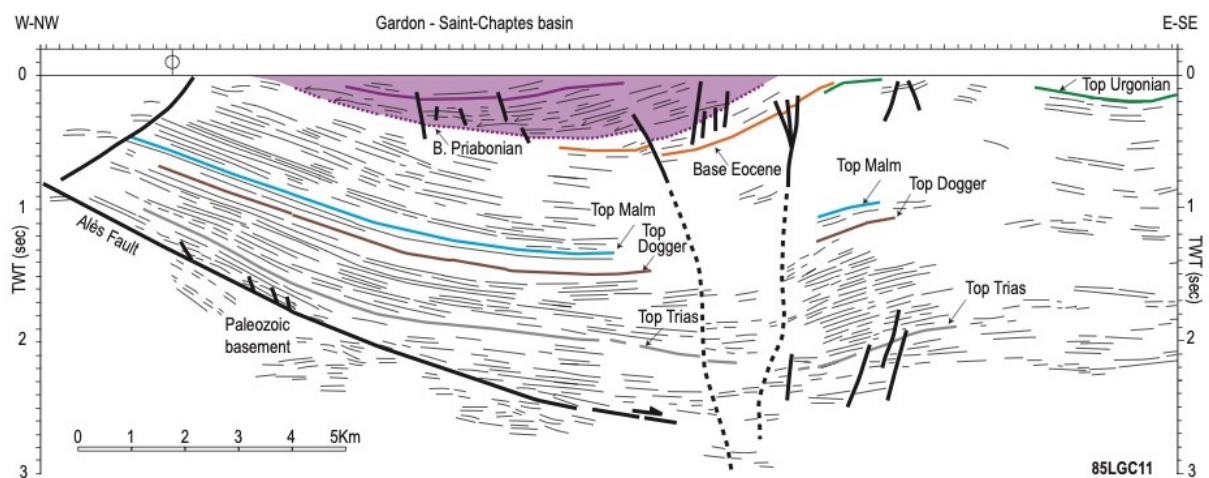
687

## 688 7. Seismic sequence analysis in the Gardon - Saint-Chaptès basin

689

690 The Priabonian Gardon - Saint-Chaptès basin (GSCB) sits at the junction of an almost  
 691 continuous NE-trending strip of Priabonian outcrops from the foreland of the Montpellier thrust  
 692 (Fig. 2), to the large syn-rift Alès basin, parallel to the NE-trending Cévennes Fault. Syn-rift  
 693 Oligocene sediments are observed, unconformable over the Priabonian, in the Alès Basins  
 694 (Sanchis and Séranne, 2000) and in a distinct outcrop in the southern part of the GSCB  
 695 (Lettéron et al., 2018). Transgression of the post-rift Burdigalian tidal sequences, restricted to  
 696 the E-W paleo-ria of Uzès basin (Reynaud et al., 2006), did not reach the Alès basin. The  
 697 Gardon segment, between Alès and Saint-Chaptès, consists of a large asymmetrical syncline,  
 698 with a distinctive NW-trend, contrasting with the general NE-trend of the contemporaneous  
 699 basins (Fig. 2).

700 Pyrenean structures in this area consist of a succession of E-W folds affecting the thick  
 701 Triassic to Neocomian sequence (Arthaud and Laurent, 1995), dated with syn-tectonic  
 702 Paleocene to Bartonien terrigenous sediments in the syncline axes. The later are buried to the  
 703 west beneath Priabonian and Oligocene sequences, which provides a first-order evidence for  
 704 a major post-Pyrenean discontinuity (Fig.2). Detailed mapping of the northeastern border of  
 705 the GSCB also defines a marked angular unconformity of the Priabonian over the syn-  
 706 pyrenean breccia sequences (Sanchis, 2000).



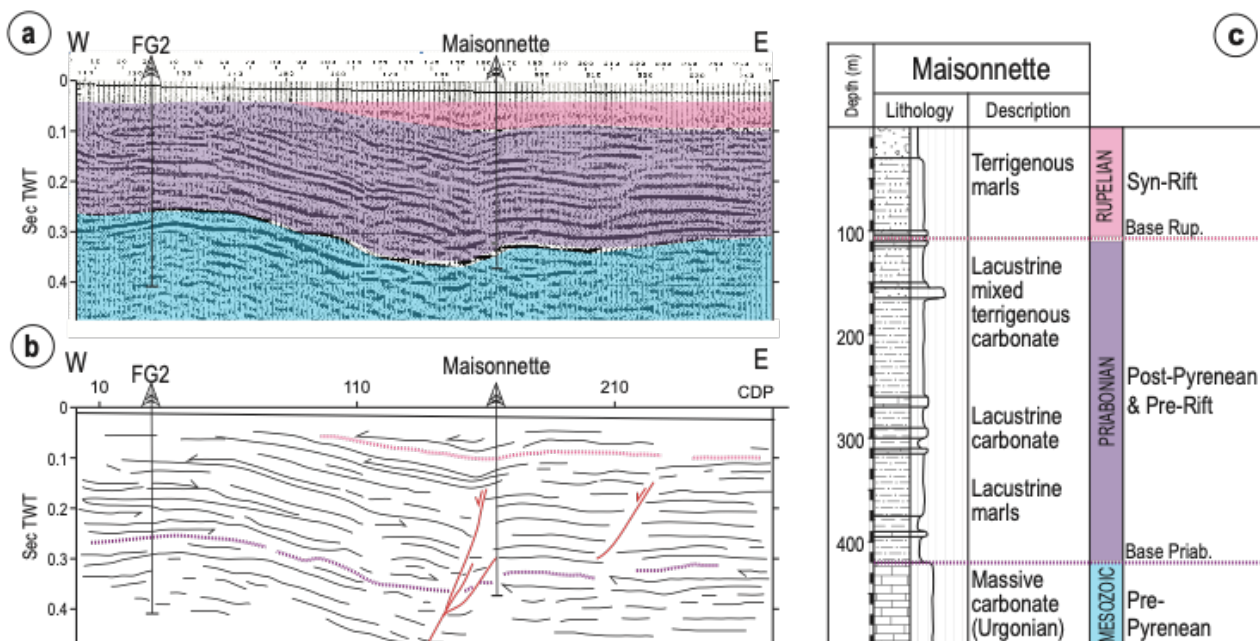
707

708 **Fig.19:** Interpreted line drawing of a seismic reflection profile across the Gardon Basin showing the syn-  
 709 depositional migration of the hanging-wall syncline. Modified after (Sanchis, 2000). Main markers are

710 identified; Priabonian interval in purple overlay; intra-Priabonian marker corresponds to the base of  
 711 “Grès de Celas” Formation. Location on Fig. 2 and 21.

712

713 Chronostratigraphy is rather well constrained due to numerous mammalian fossils (Fig. 3)  
 714 reviewed in (Lettéron et al., 2018). Priabonian deposits form a wide asymmetric syncline,  
 715 including a thick NE and reduced SW limbs, respectively. Seismic reflection survey of the Alès  
 716 basin included a southern profile (85LGC11), which reveals the structure and mode of  
 717 formation of this syncline (Sanchis, 2000) (Fig. 19). In section, the GSCB displays Priabonian  
 718 growth syncline migrating WNW-ward, which characterises dip-slip movement of a hanging-  
 719 wall flat made of Mesozoic sequence detached above an eastward, low-dipping, decollement,  
 720 above the Paleozoic basement. Such low-dipping decollement, the “Alès Fault”, has been  
 721 identified in the neighbouring Alès basin and beneath the Mesozoic sequence, folded during  
 722 the Pyrenean (Benedicto, 1996; Sanchis, 2000; Sanchis and Séranne, 2000). This  
 723 decollement at the basement-cover interface is distinct from the Cévennes basement fault,  
 724 although both the Cévennes and Alès faults emerge along the same trace. This seismic profile  
 725 (Fig. 19) also provides evidence for 4km E-SE migration of the depocentre, therefore  
 726 suggesting similar displacement of the hanging-wall across the Alès Fault, in this direction,  
 727 during Priabonian.



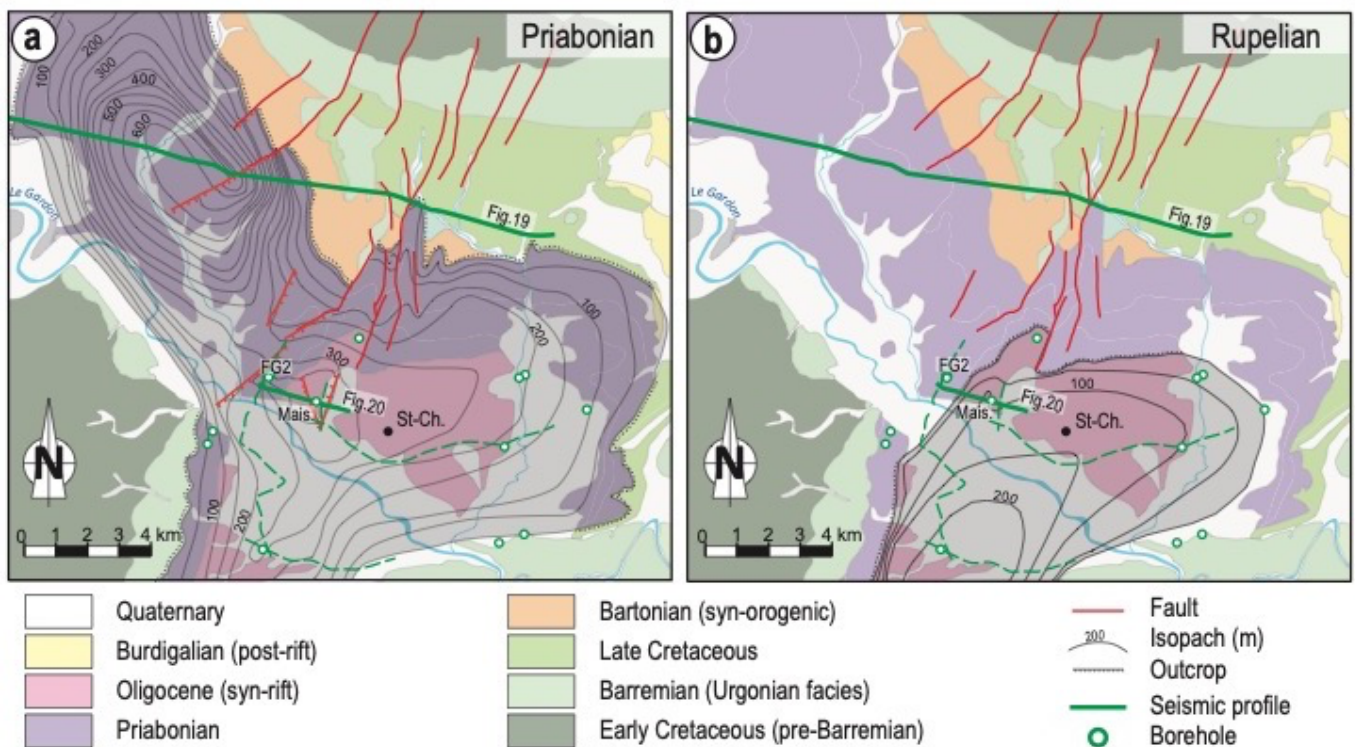
728

729 **Fig. 20:** Seismic reflection profile and corresponding line drawing in the Gardon - Saint-Chaptes basin  
 730 showing evidence for syn-depositional (Priabonian) extensional faulting sealed by the Rupelian  
 731 sequence. Maisonnette borehole allows to interpret and to date the sequence. Modified after (Baral,  
 732 2018). Location on Fig. 2 and 21.

733



734 The Saint-Chaptes part of the GSCB has been investigated by seismic reflection profiling,  
 735 aiming at hydrogeological exploration of the covered Barremian *Urgonian* karst (Josnin, 2001).  
 736 The sections tied to 4 wells sampling the Oligocene and Priabonian interval (Fig. 2) (Baral,  
 737 2018; Baral et al., 2018) and correlated with surface exposures providing sedimentology and  
 738 stratigraphy controls (Lettéron et al., 2018), allowed to identify, date and map the major seismic  
 739 markers across the basin (Fig. 20). In borehole, the Priabonian sequence consists of lacustrine  
 740 marls and carbonates, that pass upward to sandstones. It rests on a thin interval of undated  
 741 detrital continental sediment, which can be tentatively correlated with the syn-tectonic  
 742 Bartonian observed in outcrops north of the borehole. Priabonian displays growth structures  
 743 generated by extensional faults which ramp down into the Barremian (*Urgonian* facies)  
 744 massive limestones. Such faults belong to the N-NE trending fault-network that truncates the  
 745 Pyrenean folds, and is sealed by the Rupelian syn-rift sequence (Fig. 2). The dip-slip  
 746 component of such faults observed in seismic, is not associated with any significant horizontal  
 747 displacement, since the pyrenean fold axes (Berger et al., 1978) are not laterally offset (Fig.  
 748 2).



7  
 750 **Fig. 21:** Isopach maps of Priabonian (a) and Rupelian (b) sequences in the Gardon – Saint-Chaptes  
 751 basin. Note the different orientation of the Rupelian depocentre axis with respect to the previous  
 752 Priabonian subsidence axis. Location in Fig. 2.

753  
 754 Time-depth conversion was achieved using velocities stack provided with the seismic profiles  
 755 and controlled with the borehole data (Baral, 2018), in order to make an isopach maps of the

756 Priabonian depocentre Fig. 21a). It provides evidence for Priabonian tectonics across N-NE-  
 757 trending active faults, observed north of the basin, and southward, parallel to the Sommières  
 758 basin (Fig. 2). The Gardon segment of the depocentre, although less well constrained by  
 759 subsurface data, designs the NNW-trending asymmetrical syncline imaged in seismic (Fig.  
 760 19). The overlying Oligocene (syn-rift) depocentre (Fig.21b) is restricted to the Saint-Chaptes  
 761 part of the GSCB and it is not affected by the earlier faults, nor controlled by any active  
 762 boundary faults. It designs a wide depocentre, whose subsidence axis strikes N050, oblique  
 763 with respect with the Priabonian depocentre. This suggests a Rupelian syn-rift basin formed  
 764 as a hanging-wall syncline (Benedicto et al., 1999) above a detachment, which we interpret to  
 765 be the Paleozoic basement-Mesozoic cover interface, i.e. the Alès Fault in this area. The  
 766 structural relationships in the GSCB and the contrasted orientation of the Priabonian and  
 767 Rupelian depocentres indicate two distinct events with different extension directions.

768

## 769 **8. Regional synthesis and discussion**

770

771 Field observations show that the GB, LMB and SMLB display similar Paleogene successions  
 772 and stratigraphic settings. In all exposed basins, the syn-tectonic pyrenean continental  
 773 formations consist of breccia along the active thrusts that pass distally, i.e. northwards, to fine  
 774 continental silts and marls, or lacustrine/palustrine limestones. They are overlain by Priabonian  
 775 continental sediments, which were deposited in alluvial floodplains, including channelized  
 776 polygenic, sub-rounded, conglomerates. Proximal-distal facies distributions, paleocurrents and  
 777 some distinctive clast lithologies are consistent with a southern source for the clastic  
 778 sediments. This is related with a remaining pyrenean topography that extended in the present-  
 779 day Gulf of Lion, until the Priabonian. Priabonian formations are preserved in distinct basins or  
 780 sub-basins corresponding to subsiding depocentres, which display significant thickness  
 781 variations and syn-tectonic growth structures. The lower boundary is an unconformity over the  
 782 pyrenean syn-orogenic formations and structures, although it can locally be observed  
 783 conformable at outcrop scale. The angular unconformity is better expressed where pyrenean  
 784 tectonics was more developed: i.e. close to the Montpellier and Pic-Saint-Loup thrusts and  
 785 around the anticlines. Priabonian sequences are eroded and unconformably overlain by Late  
 786 Rupelian continental alluvial fans and lacustrine deposits, in relation with the rifting of the Gulf  
 787 of Lion margin, except in the SMLB, where the stratigraphic record ends with Priabonian. The  
 788 Priabonian sequences of the GSCB, observed in seismic profile and tied to borehole data, and  
 789 those from the HB (although not precisely dated) provides evidence for similar structural and  
 790 stratigraphic relationships, as observed in the field. Pyrenean structures and syn-orogenic  
 791 sequences are unconformably overlain by a seismic sequence of highly variable thickness,  
 792 which is also truncated by younger sequences displaying syn-rift growth structures against the

793 basin bounding normal faults. We correlate this intermediate seismic sequence with the  
 794 Priabonian interval described in the field in GB, LMB and SMLB.

795 At variance with the observed similar structural relationship with underlying and overlying  
 796 sequences, the Priabonian deposits display contrasting structures in the different basins  
 797 investigated (Fig. 22):

798

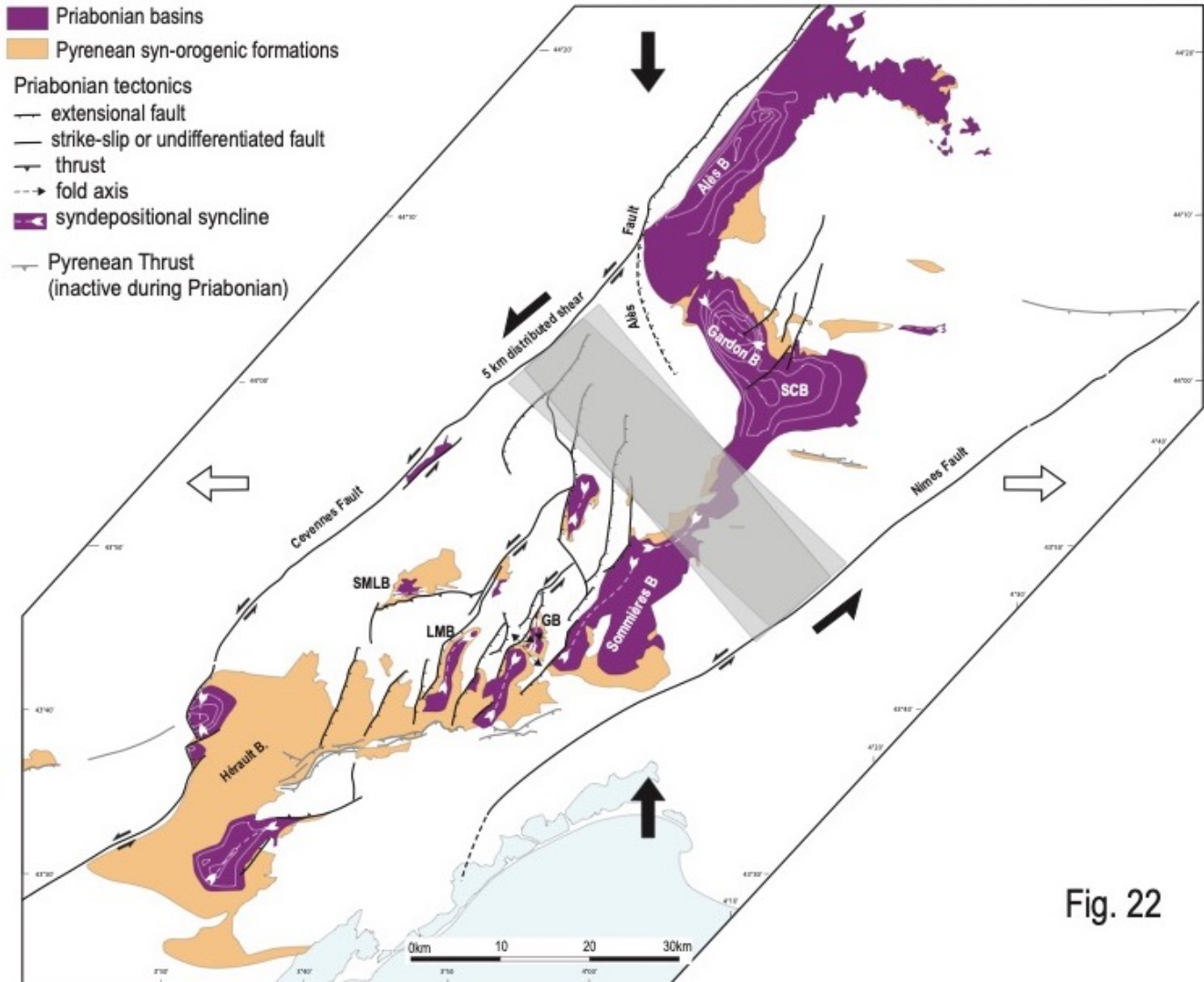


Fig. 22

799  
 800 **Fig. 22:** Synthetic regional map of Priabonian structures and kinematics in Languedoc. For location of  
 801 specific features and localities, please refer to Fig. 2, which shares the same frame. The study area  
 802 corresponds to a zone of sinistral shearing between the Cévennes and Nîmes faults, with a minimal  
 803 value of 5 km (grey overlay symbolises the simple shear).

804

- 805 - LMB: Syn-tectonic growth-structures are consistent with a hanging-wall syncline,  
 806 resulting from extensional faulting along the NNE-striking bounding normal fault.
- 807 - SMLB: Structures are related to syn-depositional compressional folding across the E-  
 808 trending Pic-Saint-Loup thrust.

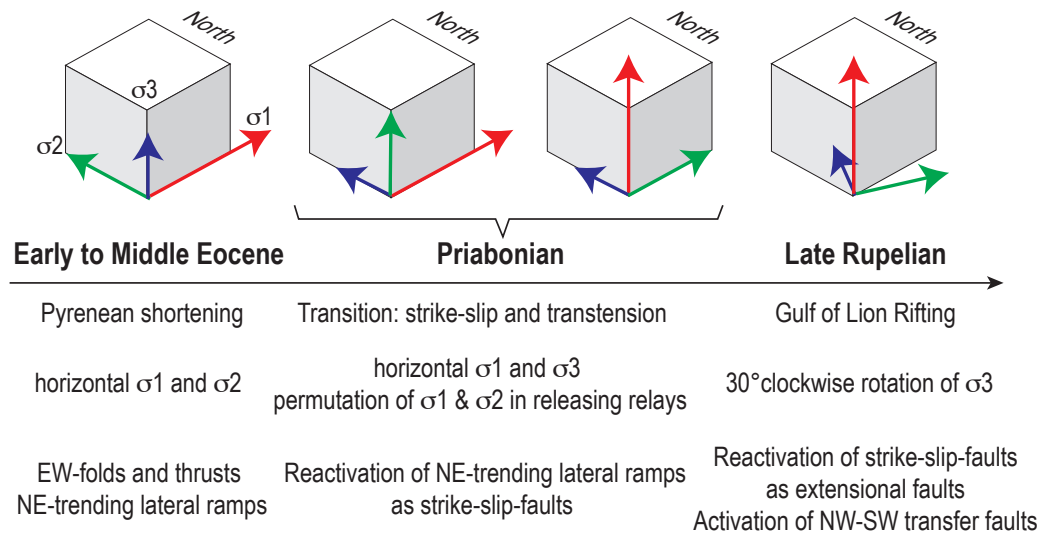


- 809 - GB: The tectonic sketch derived from the detailed geological map Fig.7 displays syn-  
810 depositional folding, which characterises both NE-SW compression and EW extension;  
811 in addition, there is evidence of left-lateral strike-slip along NNE-trending faults (Fig.  
812 11b).
- 813 - HB: Depocentre distribution with respect with controlling faults suggests left-lateral  
814 motion along the NNE-trending Cévennes Fault, which accommodates normal faulting  
815 across N-trending splays (Fig. 22).
- 816 - GSCB: The Priabonian sequence was deposited as a hanging-wall syncline controlled  
817 by a SE-trending extensional low-angle decollement of the Mesozoic cover over the  
818 Paleozoic basement.

819 Such apparently contradicting kinematics can be understood in an overall left-lateral  
820 deformation along the regional NNE-trending faults, such as the Cevennes, Les-Matelles-  
821 Corconne and the Nîmes faults (Fig.22). When submitted to a stress regime characterised by  
822 a horizontal, N-S, maximum principal stress  $\sigma_1$  and a horizontal E-W minimum principal stress  
823  $\sigma_3$ , inherited faults oriented NNE are reactivated as left-lateral strike-slip faults, with restraining  
824 bends (Christie-Blick and Biddle, 1985) along more northerly oriented segments, as in LMB,  
825 HB, GSCB. East-west oriented fault splays such as the Pic-Saint-Loup correspond to  
826 restraining bends. Syn-tectonic deposition in the syncline north of Uzès (Fig.2, Fig.22) also  
827 provide additional evidence for N-S shortening across EW oriented structures, during  
828 Priabonian.

829 The amount of left-lateral displacement during Priabonian is poorly constrained, as it  
830 reactivates, and is superimposed, onto Pyrenean left-lateral ramps, resulting in a combined  
831 finite strain, which hampers the distinction of the two contributions to the strike-slip offset. In  
832 addition, our study shows that i) the strain was distributed across the whole area between the  
833 Cévennes and Nîmes faults and ii) possible discrepancies between the amount of deformation  
834 recorded in the Mesozoic cover and the basement may occur. However, the Priabonian  
835 tectonic-sedimentation relationships recorded in some of the studied basins provide minimum  
836 values for the offset. The extensional growth structure in the Hérault basin (Fig. 16 c) suggests  
837 a minimum extension of some 3 km, corresponding to the minimum value of Priabonian left-  
838 lateral offset across this segment of the Cévennes fault. The migration of the Priabonian  
839 hanging-wall syncline in the GSCB (Fig. 19) indicates NE-ward displacement of 4 km.  
840 Restoration of the LMB points to 375m Priabonian extension (Benedicto et al., 1999) across a  
841 releasing bend of the Matelles-Corconne Fault. This could represent the order of magnitude of  
842 displacement across the other identified NE-trending faults that bound the Guzargues and  
843 Sommières basins (Fig. 2). We thus suggest that the Priabonian cumulated left-lateral motion  
844 distributed across the 40 km wide NE-trending wrenching zone remained moderate, with a  
845 minimal value of 4 to 5 kilometres. Even though some wrenching may have occurred without

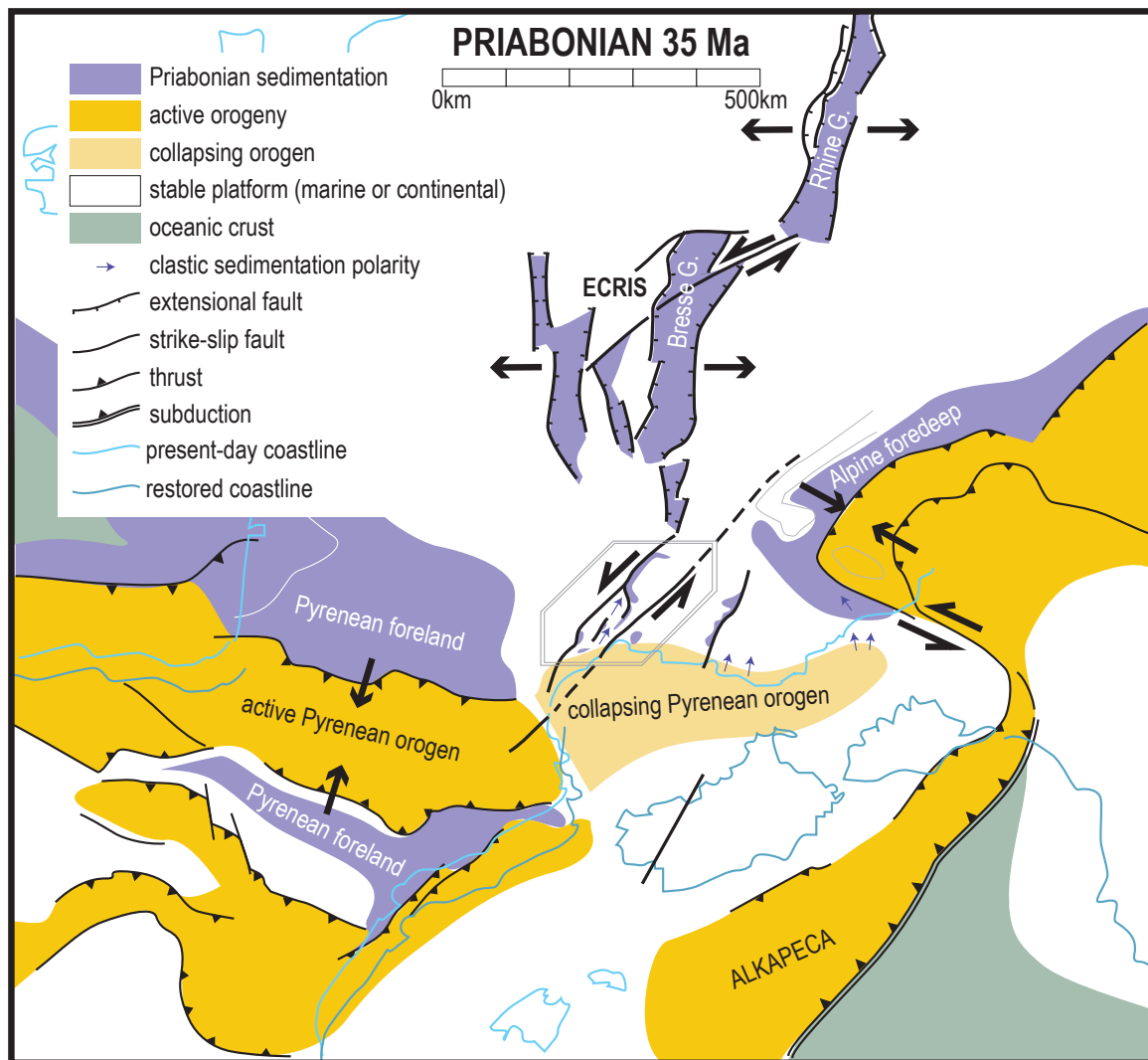
846 any syn-tectonic deposits recorded, the cumulated Priabonian movement unlikely exceeded  
 847 10km. There is no data to document the offset across the major Nîmes fault.



848  
 849 **Fig. 23:** Evolution of stress regime from mid-Eocene Pyrenean shortening, through Priabonian strike-  
 850 slip regime, to Rupelian rifting.

851  
 852 The transition from Pyrenean compressional mountain building to rifting of the Gulf of Lion in  
 853 Languedoc was achieved by a specific evolution of the stress regime (Fig. 23). From latest  
 854 Cretaceous to Bartonian the N-S convergence of Sardinia and associated continental block  
 855 with southern Europe was accommodated by E-W folds and thrusts, while the inherited  
 856 regional NE-trending faults were activated as lateral-ramps. Such deformation results from a  
 857 horizontal  $\sigma_1$  oriented N-S and a vertical  $\sigma_3$  (Arthaud and Laurent, 1995). During Priabonian,  
 858 the stress regime evolved by permutation of  $\sigma_2$  and  $\sigma_3$  axes,  $\sigma_1$  remaining horizontal and  
 859 oriented N-S. Such stress regime activated the inherited NE-trending faults as left-lateral  
 860 strike-slip faults. This fault network inherited from the Late Cretaceous-Bartonian Pyrenean  
 861 orogeny included restraining and releasing relays, the later correspond to Priabonian  
 862 depocentres, where  $\sigma_1$  and  $\sigma_2$  permuted. The restraining bend, where compression occurred  
 863 ( $\sigma_1$  N-S horizontal and  $\sigma_3$  vertical) is illustrated by the Saint-Martin de Londres basins.  
 864 Contemporaneous releasing bend and relay, where local extension occurred ( $\sigma_1$  vertical) is  
 865 exemplified by the northern part of the Hérault basin, Les-Matelles basin, or Gardon Saint-  
 866 Chaptes basin. (Fig. 22). Permanence of N-S horizontal  $\sigma_1$  from Late Cretaceous through to  
 867 Late Eocene was also documented in southern Provence, defined by both strike-slip or reverse  
 868 faults (Lacombe et al., 1992). N-S shortening along the regional NE-trending faults  
 869 accommodated transpression of the oblique Africa-Eurasia convergence in the Languedoc-  
 870 Provence-Corsica domain (Lacombe and Jolivet, 2005) and lasted until Priabonian. During  
 871 Late Rupelian, the stress regime rotated clockwise around the vertical  $\sigma_1$ , by 30° (Séranne,

872 1999), which activated the inherited NE-trending strike-slip faults as extensional faults. This  
 873 Rupelian change in stress orientation reflects a change at plate boundaries, which we relate  
 874 to the onset of subduction roll-back and back-arc rifting above the Apennine subduction (Jolivet  
 875 and Faccenna, 2000; Jolivet et al., 2015; Réhault et al., 1984; Romagny et al., 2020; Séranne,  
 876 1999). Southeast-trending transfer faults zones are a distinctive feature of the rifting of the Gulf  
 877 of Lion (Canva et al., 2020; Gorini et al., 1993; Guennoc et al., 2000; Maillard et al., 2020;  
 878 Mauffret et al., 2001). However, there is no evidence of active SE-oriented structure in the  
 879 onshore study area, until the Oligocene rifting episode (Maerten and Séranne, 1995; Sanchis  
 880 and Séranne, 2000). The Priabonian strike-slip deformation documented in the present study  
 881 therefore constitutes a distinct tectonic phase, corresponding to different kinematics and  
 882 driving forces than the rifting of the Gulf of Lion (Séranne, 1999). We suggest that the  
 883 development of SE trending transfer zones in the back-arc basin, as from the Rupelian, dates  
 884 the initiation of slab tearing in the underlying subduction zone (Romagny et al., 2020).



885

886 **Fig. 24:** Simplified map Pyrenees / European Cenozoic Rift System / Alps during Priabonian.

887 *Paleogeographic reconstruction at 35 Ma from (Romagny et al., 2020); Position of the North Alpine*  
 888 *foreland from (Dumont et al., 2012; Ford and Lickorish, 2004) and of the ECRIS from (Dèzes et al.,*  
 889 *2004).*

890

891 Priabonian left-lateral wrenching in Languedoc links the active Pyrenean orogen to the E-W  
 892 rifting of the European Cenozoic Rift System (ECRIS) (Dèzes et al., 2004) and the North Alpine  
 893 Foreland Basin (Ford and Lickorish, 2004). Such left-lateral wrenching during Priabonian most  
 894 probably extended southward in the Corbières (Fig. 1); however, lack of Priabonian  
 895 sedimentary record in this area does not allow to confirm this. Eocene northward motion of the  
 896 Adriatic plate was accommodated by left-lateral oblique convergence along the SW Alps until  
 897 continental collision in Oligocene (Dumont et al., 2012; Ford et al., 2006) (Fig. 24).  
 898 Convergence between the Iberia and Europe respectively lasted until early Miocene in the  
 899 Pyrenees e.g. (Mouthereau et al., 2014; Teixell et al., 2018) and *circa* 85km shortening is  
 900 computed for the Late Eocene to Early Oligocene interval (Teixell et al., 2016). Pyrenean  
 901 shortening in Corbières, Languedoc and Provence terminated during the Bartonian  
 902 (Alabouvette et al., 2001; Bestani et al., 2015; Séguret and Benedicto, 1999). Northward  
 903 flowing clastic sedimentation pattern in Languedoc, Provence and the SE Alps shows that this  
 904 segment of the orogen, located in the present-day Gulf of Lion, was being dismantled at that  
 905 time (Egerton, 1996; Guieu and Roussel, 1990; Joseph and Lomas, 2004).

906 The left-lateral movement along the Nîmes and Cévennes fault system extended northward to  
 907 the Jura region where sinistral strike-slip is well documented during Eocene (Hombert et al.,  
 908 2002). It is also consistent with the transfer zone between Rhine and Bresse grabens (Bergerat  
 909 et al., 1990; Lacombe et al., 1993; Madritsch et al., 2009), which both record a distinctive  
 910 Priabonian pulse of sedimentation predating a mid-Oligocene extensional tectonics (Sissingh,  
 911 1998). Crustal extension across these rift basin amounts to 7 km (Ziegler and Dèzes, 2005), a  
 912 value in agreement with the offset measured across the strike-slip faults.

913 During the Priabonian, the Languedoc-Provence segment of the Pyrenean orogen was thus  
 914 surrounded by two active convergence zones, while it was undergoing collapse. This different  
 915 behaviour may be due to the interaction with the west-European rifting (Dèzes et al., 2004),  
 916 which propagated southward beneath the Languedoc-Provence-Pyrenees.

917

## 918 **9. Conclusion**

919

920 The transition from the Pyrenean orogeny to the Gulf of Lion rifting in onshore Languedoc  
 921 occurred during Priabonian. Prior to Priabonian time, every structural and tectonic-  
 922 sedimentation evidence argue for pyrenean compressional deformation. In contrast, after

923 Priabonian, all structures indicate NW-SE extension related to the Gulf of Lion rifting. This  
924 makes the Priabonian interval a key intermediate period of kinematic change. Reassessment  
925 of the chronostratigraphic evolution of the area allowed us to constrain the calendar of events.  
926 This period is recorded by deposition of a distinctive sedimentary sequence, which is  
927 documented both by surface analyses and seismic profiling of Priabonian basins. Such  
928 intermediate sequence is bounded at the base by an angular unconformity over the Pyrenean  
929 structures, and at the top by the Oligocene syn-rift unconformity, respectively. Continental  
930 sedimentation ranges from lacustrine/ palustrine limestone and evaporitic marls at the base,  
931 to marls and silts of alluvial plain, including variable proportion of sandstone sheets and  
932 channelised fluvial conglomerates, toward the top. The Priabonian series progrades north- or  
933 northeastward and is derived from a southern source, presently located offshore, which  
934 indicates the existence of a remaining pyrenean topography in the present-day Gulf of Lion.

935 Mapping and seismic analyses of the tectonic-sedimentation relationships in the Priabonian  
936 basins give evidence for syn-depositional deformation against bounding faults and in growth  
937 synclines. Contrasted modes of deformation are observed, within short distance, in the  
938 Priabonian basins: i) controlled by extensional movement of NNE to NNW-trending faults or  
939 segments of faults or ii) controlled by E-W-oriented thrusts and folds. Regional mapping of  
940 these structures shows a distribution of the compressional and extensional structures which  
941 are consistent with a left-lateral shearing of the area comprised between the major, NE-  
942 trending, Cévennes and Nîmes faults. Such sinistral strike-slip of moderate offset ( $\pm 5$  km)  
943 accommodates the E-W extension of the West European rifts basins that are located to the  
944 north of the study area. To the south, the strike-slip faults are connected to the ongoing  
945 shortening in the Spanish Pyrenees. Priabonian deformation and sedimentation records the  
946 initial stages of the dismantling of the Languedoc-Provence segment of Pyrenees, located  
947 between two active orogens: the Spanish Pyrenees and the Western Alps. The late orogenic  
948 dismantling of the eastern Pyrenees (Jolivet et al., 2020) therefore started up to 5 My earlier  
949 than the Rupelian onset of Apennine subduction retreat and associated back-arc NW-SE  
950 extension.

951

#### 952 **Acknowledgements:**

953 This study was carried out during the OROGEN project, funded by TOTAL, BRGM and CNRS-  
954 INSU. It benefited from the stimulating discussions amongst the OROGEN community.  
955 We acknowledge the BRGM for providing the reprocessed lines of the H83 and H84 seismic  
956 surveys, presented in this study. We are indebted to SMAGE (*Syndicat Mixte pour*

957 *l'Aménagement et la Gestion Equilibrée des Gardons*) for providing us with subsurface data  
 958 for the Gardon Saint-Chaptes basin, and for support for C.B.

959 We are extremely grateful to J.Y. Crochet, J.A. Remy, F. Lihoreau, and R. Tabuce (ISEM-  
 960 University of Montpellier) for discussing palaeontology and mammal biostratigraphy, and for  
 961 guiding us to the precise locations of ancient and more recent paleontological discoveries.

962 The paper benefited from fruitful exchanges with Flavia Girard and Renaud Caby  
 963 (Géosciences Montpellier), François Fournier (CEREGE), Alexandre Letteron (IFP-CEREGE),  
 964 Hubert Camus (Cenote) and Pascal Fénart (Hydrofifis).

965 The manuscript has been improved (and extended!) thanks to the insightful comments of  
 966 François Guillocheau, Sylvain Calassou, and of an anonymous reviewer. The precious  
 967 suggestions and corrections of the Guest Editor, Olivier Lacombe, are greatly appreciated.

## 968 **References**

- 969 Aguilar, J. P., Legendre, S., and Michaux, J., 1997, Actes du Congrès Biochrom'97 - Montpellier, 14-17 Avril 1997:  
 970 Montpellier, p. 818p.
- 971 Alabouvette, B., Arthaud, F., Feist, R., Medioni, R., and Brousse, R., 1982, Carte Géologique de la France au 1/50  
 972 000. Feuille de Lodève: BRGM.
- 973 Alabouvette, B., Berger, G., Demange, M., and Guérangé-Lozes, J., 2001, Montpellier - Carte Géologique de la  
 974 France à 1/250000ème: BRGM.
- 975 Andrieux, J., Mattauer, M., Tomasi, P., Martinez, C., Reille, J. L., Matte, P., Bousquet, J. C., Raouf, K. A., Bel, F.,  
 976 Verrier, J., Bonnet, M., and Sauvel, M., 1971, Carte Géologique de la France au 1/50 000. Feuille de  
 977 Montpellier N° 990 BRGM.
- 978 Arthaud, F., and Laurent, P., 1995, Contraintes, déformation et déplacement dans l'avant-pays Nord-pyrénéen du  
 979 Languedoc méditerranéen: *Geodynamica Acta*, v. 8, p. 142-157.
- 980 Arthaud, F., Mégard, F., and Séguret, M., 1977, Cadre tectonique de quelques bassins sédimentaires: *Bull. Centres*  
 981 *Explor.-Prod. Elf Aquitaine*, v. 1, no. 1, p. 147-188.
- 982 Arthaud, F., Ogier, M., and Séguret, M., 1981, Géologie et géophysique du Golfe du Lion et de sa bordure nord:  
 983 *Bulletin du BRGM*, v. (2),1, no. 3, p. 175-193.
- 984 Arthaud, F., and Séguret, M., 1981, Les structures pyrénéennes du Languedoc et du Golfe du Lion (Sud de la  
 985 France): *Bulletin de la Société Géologique de France*, v. XXIII, no. 1, p. 51-63.
- 986 Baral, C., 2018, Caractérisation géologique du réservoir karstique profond du bassin de Saint-Chaptes, Gard,  
 987 France [Master 2: Montpellier, 50 p.
- 988 Baral, C., Séranne, M., Fénart, P., and Camus, H., Geological characterization and formation of a covered karstic  
 989 reservoir in the Urgonian limestones of the Saint Chaptes Basin (Gard, South of France): towards  
 990 predicting the distribution and state of karstification, *in Proceedings Eurokarst 2018*, Besançon, France,  
 991 2- 5 juillet 2018 2018.
- 992 Barrier, L., Proust, J.-N., Nalpas, T., Robin, C., and Guillocheau, F., 2010, Control of alluvial sedimentation at  
 993 foreland-basin active margins: a case study from the Northeastern Ebro basin (Southeastern Pyrenees,  
 994 Spain): *Journal of Sedimentary Research*, v. 80, p. 728-749.
- 995 Benedicto, A., 1996, Modèles tectono-sédimentaires de bassins en extension et style structural de la marge passive  
 996 du Golfe du Lion (Partie Nord), sud-est de la France: Université de Montpellier II.
- 997 Benedicto, A., Labaume, P., Séguret, M., and Séranne, M., 1996, Low-angle crustal ramp and basin geometry in  
 998 the Gulf of Lion passive margin: the Oligocene-Aquitainian Vistrenque graben, SE France: *Tectonics*, v.  
 999 15, no. 6, p. 1192-1212.
- 1000 Benedicto, A., Séguret, M., and Labaume, P., 1999, Interaction between faulting, drainage and sedimentation in  
 1001 extensional hanging-wall syncline basins: example of the Oligocene Matelles Basin, Gulf of Lion margin  
 1002 (S.E. France), *in Durand, B., Jolivet, L., Horváth, F., and Séranne, M., eds., The Mediterranean Basins :*  
 1003 *Tertiary extension within the Alpine Orogen*, Volume Special Publication 156: London, The Geological  
 1004 Society, p. 81-108.

- 1005 Berger, G., Feist, R., and Freydet, P., 1981, Carte Géologique de la France au 1/50 000. Feuille de Pézenas: BRGM.
- 1006 Berger, G., Lemprière, P., and Séguret, M., 1978, Carte Géologique de la France au 1/50 000. Feuille d'Anduze
- 1007 n°938: BRGM.
- 1008 Bergerat, F., Mugnier, J.-L., Guellec, S., Truffert, C., Cazes, M., Damotte, B., and Roure, F., 1990, Extensional
- 1009 tectonics and subsidence of the Bresse basin: an interpretation from ECORS data: *Mémoire de la Société*
- 1010 *Géologique de France*, v. 156, p. 145-156.
- 1011 Bestani, L., 2015, *Géométrie et cinématique de l'avant-pays provençal : Modélisation par coupes équilibrées dans*
- 1012 *une zone à tectonique polyphasée*. [PhD Doctorat]: Université Aix-Marseille, 244 p.
- 1013 Bestani, L., Espurt, N., Lamarche, J., Bellier, O., and Hollender, F., 2016, Reconstruction of the Provence Chain
- 1014 evolution, southeastern France: *Tectonics*, v. 35, no. 6, p. 1506-1525.
- 1015 Bestani, L., Espurt, N., Lamarche, J., Floquet, M., Philip, J., Bellier, O., and Hollender, F., 2015, Structural style
- 1016 and evolution of the Pyrenean-Provence thrust belt, SE France: *Bulletin de la Société Géologique de*
- 1017 *France*, v. 186, no. 1LP: *Lithosphere dynamics of sedimentary basins: The Circum-Mediterranean Basins*
- 1018 *and Analogues* p. 223-241.
- 1019 Canva, A., Thion, I., Peyrefitte, A., Couëffé, R., Maillard, A., Jolivet, L., Martelet, G., Lacquement, F., and
- 1020 Guennoc, P., 2020, The Catalan magnetic anomaly: Its significance for the crustal structure of the Gulf of
- 1021 Lion passive margin and relationship to the Catalan transfer zone: *Marine and Petroleum Geology*, v. 113,
- 1022 p. 104174.
- 1023 Chelalou, R., Nalpas, T., Bousquet, R., Prevost, M., Lahfid, A., Poujol, M., Ringenbach, J.-C., and Ballard, J.-F.,
- 1024 2016, New sedimentological, structural and paleo-thermicity data in the Boucheville Basin (eastern North
- 1025 Pyrenean Zone, France): *Comptes Rendus Géosciences*, v. 348, no. From rifting to mountainbuilding:
- 1026 *the Pyrenean Belt*, p. 312-321.
- 1027 Chevrot, S., Sylvander, M., Diaz, J., Martin, R., Mouthereau, F., Manatschal, G., Masini, E., Calassou, S., Grimaud,
- 1028 F., Pauchet, H., and Ruiz, M., 2018, The non-cylindrical crustal architecture of the Pyrenees: *Scientific*
- 1029 *Reports*, v. 8, p. 9591.
- 1030 Christie-Blick, N., and Biddle, K. T., 1985, Deformation and basin formation along strike-slip, *in* Christie-Blick, N.,
- 1031 and Biddle, K. T., eds., *Strike-Slip Deformation, Basin Formation, and Sedimentation, Volume Special*
- 1032 *Publication 37*, SEPM, p. 1-34.
- 1033 Christophoul, F., Ford, M., Groot, A., Rougier, G., and Hemmer, L., Tectono-stratigraphic evolution of the
- 1034 northeastern Pyrenean Foreland, *in* *Proceedings International Geological Congress, 2016, Volume 35*, p.
- 1035 paper 3188.
- 1036 Cochelin, B., Lemirre, B., Denèle, Y., De Saint-Blanquat, M., Lahfid, A., and Duchêne, S., 2018, Structural
- 1037 inheritance in the Central Pyrenees: the Variscan to Alpine tectonometamorphic evolution of the Axial
- 1038 Zone: *Journal of the Geological Society of London*, v. 175, no. 2, p. 336-351.
- 1039 Crochet, J.-Y., Godinot, M., Hartenberger, J.-L., Rémy, J. A., Sigé, B., and Sudre, J., 1988, Découverte dans le
- 1040 bassin de Saint-Martin-de-Londres (Hérault, Sud de la France) d'un gisement à vertébrés continentaux
- 1041 d'âge Eocène moyen: *Cour. Forsch.-Inst. Senckenberg*, v. 107, p. 419-434.
- 1042 Crochet, J.-Y., Hartenberger, J.-L., Rémy, J.-A., Sudre, J., and Welcome, J.-L., 1997, Découverte de vertébrés
- 1043 continentaux de l'Eocène moyen et supérieur dans le bassin des Matelles (Hérault, Sud de la France) et
- 1044 redécouverte du "*Lophiodon* des Matelles": *Géologie de la France*, v. 1, p. 35-45.
- 1045 Crochet, J. Y., 1984, Géologie et paléontologie de la partie septentrionale du fossé oligocène des Matelles (Hérault,
- 1046 sud de la France): *Géologie de la France*, v. 1-2, p. 91-104.
- 1047 Cunningham, W. D., and Mann, P., 2007, Tectonics of strike-slip restraining and releasing bends, *in* Cunningham,
- 1048 W. D., and Mann, P., eds., *Tectonics of strike-slip restraining and releasing bends, Volume Special*
- 1049 *Publication n° 290*: London, The Geological Society, p. 1-12.
- 1050 Dautria, J.-M., Liotard, J.-M., Bosch, D., and Alard, O., 2010, 160 Ma of sporadic basaltic activity on the Languedoc
- 1051 volcanic line (southern France) : A peculiar case of lithosphere-asthenosphere interplay: *Lithos*, v. 120, p.
- 1052 202-222.
- 1053 Debrand-Passard, S., and Courbouleix, S., 1984, Synthèse géologique du Sud-Est de la France - Stratigraphie et
- 1054 paléogéographie, Orléans, France, BRGM, 615 p.:
- 1055 Debroas, E.-J., 1990, Le flysch noir albo-cénomaniem témoin de la structuration albienne à sénonienne de la Zone
- 1056 nord-pyréenne en Bigorre (Hautes-Pyrénées, France): *Bulletin de la Société Géologique de France*, v.
- 1057 VI, no. 2, p. 273-285.
- 1058 Dèzes, P., S.M., S., and P.A., Z., 2004, Evolution of the European Cenozoic Rift System: interaction of the Alpine
- 1059 and Pyrenean orogens with their foreland lithosphere: *Tectonophysics*, v. 389, p. 1-33.

- 1060 Dumont, T., Schwartz, S., Guillot, S., Simon-Labric, T., Tricart, P., and Jourdan, S., 2012, Structural and  
 1061 sedimentary records of the Oligocene revolution in the Western Alpine arc: *Journal of Geodynamics*, v.  
 1062 56-57, p. 18-38.
- 1063 Egerton, P. D., 1996, *Inherited drainage pathways sediment distribution and provenance in rift basins*[PhD]:  
 1064 University of Leeds, 386 p.
- 1065 Feist-Castel, M., 1971, Sur les Charophytes fossiles du bassin Tertiaire d'Alès (Gard): *Geobios*, v. 4, no. 3, p. 157-  
 1066 172.
- 1067 Ford, M., Duchêne, s., Gasquet, D., and Vanderhaeghe, O., 2006, Two-phase orogenic convergence in the external  
 1068 and internal SWAlps: *Journal of the Geological Society of London*, v. 163, p. 815-826.
- 1069 Ford, M., and Lickorish, W. H., 2004, Foreland basin evolution around the western Alpine Arc, *in* Joseph, P., and  
 1070 Lomas, S., eds., *Deep-Water Sedimentation in the Alpine Basin of SE France: New perspectives on the*  
 1071 *Grbs d'Annot and related systems*, Volume Special Publication 221: London, The Geological Society, p.  
 1072 39-63.
- 1073 Ford, M., and Vergés, J., 2020, Evolution of a salt-rich transtensional rifted margin, eastern North Pyrenees, France:  
 1074 *Journal of the Geological Society*, v. 178, no. 1, p. paper 2019-2157.
- 1075 Freytet, P., 1971, Les dépôts continentaux et marins du Crétacé supérieur et des couches de passage à l'Eocène  
 1076 en Languedoc: *Bulletin du BRGM*, v. 4, p. 1-54.
- 1077 Gastaud, J., Campredon, R., and Féraud, G., 1983, Les systèmes filoniens des Causses et du Bas Languedoc  
 1078 (Sud de la France) : géochronologie, relations avec les paléocontraintes: *Bulletin de la Société Géologique*  
 1079 *de France*, v. (7) XXV, no. 5, p. 737-746.
- 1080 Gaviglio, P., and Gonzales, J.-F., 1987, Fracturation et histoire tectonique du bassin de Gardanne (Bouches-du-  
 1081 Rhone): *Bulletin de la Société Géologique de France*, v. 8, no. 4, p. 675-682.
- 1082 Gorini, C., Le Marrec, A., and Mauffret, A., 1993, Contribution to the structural and sedimentary history of the Gulf  
 1083 of Lions (western Mediterranean), from the ECORS profiles, industrial seismic profiles and well data:  
 1084 *Bulletin de la Société Géologique de France*, v. 164, no. 3, p. 353-363.
- 1085 Gorini, C., Mauffret, A., Guennoc, P., and Le Marrec, A., 1994, Structure of the Gulf of Lions (Northwest  
 1086 Mediterranean Sea): A review, *in* Mascle, A., ed., *Hydrocarbon and petroleum geology of France*, Volume  
 1087 Special Publication of the European Association of Petroleum Geology No4: Berlin, Springer-Verlag, p.  
 1088 223-243.
- 1089 Gorini, C., Viallard, P., and Deramond, J., 1991, Modèle d'inversion négative : la tectonique extensive post-nappe  
 1090 du fossé de Narbonne-Sigean (Corbières, sud de la France): *C. R. Acad. Sci. Paris*, v. 312, p. 1013-1019.
- 1091 Grambast, L., 1962, Aperçu des charophytes tertiaires du Languedoc et leur signification stratigraphique: *C. R.*  
 1092 *Somm. Soc. Géol. France*, v. 10, p. 313-314.
- 1093 Guennoc, P., Gorini, C., and Mauffret, A., 2000, Histoire géologique du Golfe du Lion et cartographie du rift oligo-  
 1094 aquitainien et de la surface messinienne: *Géologie de la France*, v. 3, p. 67-97.
- 1095 Guieu, G., and Roussel, J., 1990, Arguments for the pre-rift uplift and rift propagation in the Ligurian-Provençal  
 1096 basin (Northwestern Mediterranean) in the light of Pyrenean Provençal orogeny.: *Tectonics*, v. 9, no. 5, p.  
 1097 1113-1142.
- 1098 Hampton, M. A., and Horton, B. K., 2007, Sheetflow fluvial processes in rapidly subsiding basin, Altiplano plateau,  
 1099 Bolivia: *Sedimentology*, v. 54, p. 1121-1147.
- 1100 Hartenberger, J.-L., Sigé, B., and Sudre, J., 1969, Les gisements de vertébrés de la région montpellieraine - 1.  
 1101 Gisements éocènes: *Bulletin BRGM (2)*, v. 1, no. 1, p. 7-18.
- 1102 Hippolyte, J. C., Angelier, J., Bergerat, F., Nury, D., and Guieu, G., 1993, Tectonic-stratigraphic record of  
 1103 paleostress time changes in the Oligocene basins of the Provence, southern France: *Tectonophysics*, v.  
 1104 226, p. 15-35.
- 1105 Homberg, C., Bergerat, F., Philippe, Y., Lacombe, O., and Angelier, J., 2002, Structural inheritance and cenozoic  
 1106 stress fields in the Jura fold-and-thrust belt (France): *Tectonophysics*, v. 357, p. 137-158.
- 1107 Horton, B. K., and Schmitt, J. G., 1996, Sedimentology of a lacustrine fan-delta system, Miocene Horse Camp  
 1108 Formation, Nevada, USA: *Sedimentology*, v. 43, p. 133-155.
- 1109 Husson, E., 2013, Interaction géodynamique/karstification et modélisation géologique 3D des massifs carbonatés  
 1110 : Implication sur la distribution prévisionnelle de la karstification. Exemple des paléokarsts crétacés à  
 1111 néogènes du Languedoc montpelliérain [Doctorat Doctorat]: Université Montpellier 2, 314 p.
- 1112 Jolivet, L., and Faccenna, C., 2000, Mediterranean extension and the Africa-Eurasia collision: *Tectonics*, v. 19, no.  
 1113 6, p. 1095-1106.



- 1114 Jolivet, L., Gorini, C., Smit, J., and Leroy, S., 2015, Continental breakup and the dynamics of rifting in back-arc  
1115 basins: The Gulf of Lion margin: *Tectonics*, v. 34, p. 10.1002/2014TC003570.
- 1116 Jolivet, L., Romagny, A., Gorini, C., Maillard, A., Thion, I., Couëffé, R., Ducoux, M., and Séranne, M., 2020, Fast  
1117 dismantling of a mountain belt by mantle flow: late-orogenic evolution of Pyrenees and Liguro-Provençal  
1118 rifting: *Tectonophysics*, v. 776, p. 228312.
- 1119 Joseph, P., and Lomas, S., 2004, Deep-water sedimentation in the Alpine Foreland Basin of SE France: New  
1120 perspectives on the Grès d'Annot and related systems - An introduction, *in* Joseph, P., and Lomas, S.,  
1121 eds., *Deep-Water Sedimentation in the Alpine Basin of SE France: New perspectives on the Grès d'Annot*  
1122 *and related systems*, Volume Special Publication 221: London, The Geological Society, p. 1-16.
- 1123 Josnin, J. Y., 2001, Influence de la tectonique quaternaire sur la structure de deux aquifères karstiques du  
1124 Languedoc (France): *Eclogae geologica Helvetiae*, v. 94, p. 173-184.
- 1125 Lacombe, O., Angelier, J., Byrne, D., and Dupin, J. M., 1993, Eocene-Oligocene tectonics and kinematics of the  
1126 Rhine-Saone continental transform zone (Eastern France): *Tectonics*, v. 12, no. 4, p. 874-888.
- 1127 Lacombe, O., Angelier, J., and Laurent, P., 1992, Determining paleostress orientations from faults and calcite twins:  
1128 a case study near the Sainte-Victoire Range (southern France): *Tectonophysics*, v. 201, no. 1-2, p. 141-  
1129 156.
- 1130 Lacombe, O., and Jolivet, L., 2005, Structural and kinematic relationships between Corsica and the Pyrenees-  
1131 Provence domain at the time of the Pyrenean orogeny: *Tectonics*, v. 24, no. 1, p. TC1003.
- 1132 Lagabriele, Y., and Bodinier, J.-L., 2008, Submarine reworking of exhumed subcontinental mantle rocks: field  
1133 evidence from the Lherz peridotites, French Pyrenees: *Terra Nova*, v. 20, no. 1, p. 11-21.
- 1134 Lagabriele, Y., Labaume, P., and de Saint Blanquat, M., 2010, Mantle exhumation, crustal denudation, and gravity  
1135 tectonics during Cretaceous rifting in the Pyrenean realm (SW Europe): Insights from the geological setting  
1136 of the Iherzolite bodies: *Tectonics*, v. 29, p. TC4012, 4011-4026.
- 1137 Lajoinie, J.-P., and Laville, P., 1979, Les formations bauxitiques de la Provence et du Languedoc. Dimensions et  
1138 distribution des gisements: *Mémoire du BRGM*, v. 100, p. 146.
- 1139 Lamotte, D. F. D., Souque, C., Grelaud, S., and Robion, P., 2002, Early record of tectonic magnetic fabric during  
1140 inversion of a sedimentary basin Short review and examples from the Corbières transfer zone (France):  
1141 *Bulletin de la Société Géologique de France*, v. 172, no. 5, p. 461-469.
- 1142 Le Pichon, X., Rangin, C., Hamon, Y., Loget, N., Lin, J. Y., Andreani, L., and Flotte, N., 2010, Geodynamics of the  
1143 France Southeast Basin: *Bulletin De La Societe Geologique De France*, v. 181, no. 6, p. 477-501
- 1144 Lettéron, A., Hamon, Y., Fournier, F., Séranne, M., Pellenard, P., and Joseph, P., 2018, Reconstruction of a saline,  
1145 lacustrine carbonate system (Priabonian, St-Chaptes Basin, SE France): depositional models,  
1146 paleogeographic and paleoclimatic implications.: *Sedimentary Geology*, v. 367, p. 20-47.
- 1147 Mack, G. H., and Leeder, M. R., 1999, Climatic and tectonic controls on alluvial fan and axial fluvial sedimentation  
1148 in the Plio-Pleistocene Palomas half graben, southern Rio Grande Rift: *Journal of Sedimentary Research*,  
1149 v. 69, p. 635-652.
- 1150 Madritsch, H., Kounov, A., Schmid, S. M., and Fabbri, O., 2009, Multiple fault reactivations within the intra-  
1151 continental Rhine–Bresse Transfer Zone (La Serre Horst, eastern France): *Tectonophysics*, v. 471, p.  
1152 297-318.
- 1153 Maerten, L., and Séranne, M., 1995, Extensional tectonics of the Oligo-Miocene Hérault Basin (S France), Gulf of  
1154 Lion margin: *Bulletin de la Société Géologique de France*, no. 6, p. 739-749.
- 1155 Maillard, A., Jolivet, L., Lofi, J., Thion, I., Couëffé, R., Canva, A., and Dofal, A., 2020, Transfer zones and  
1156 associated volcanic province in the eastern Valencia Basin: Evidence for a hot rifted margin?: *Marine and*  
1157 *Petroleum Geology*, v. 119, p. 104419.
- 1158 Mascle, A., and Vially, R., 1999, The petroleum systems of the South-East Basin and Gulf of Lions (France), *in*  
1159 Durand, B., Jolivet, L., Horváth, F., and Séranne, M., eds., *The Mediterranean Basins : Tertiary extension*  
1160 *within the Alpine Orogen*, Volume Special Publication 156: London, The Geological Society, p. 121-140.
- 1161 Mattauer, M., 2002, La faille normale oligocène des Matelles (environs de Montpellier). Une difficile confrontation  
1162 entre un modèle à la mode et les observations de terrain: *Géologie de la France*, v. 1, p. 39-43.
- 1163 Mauffret, A., Durand de Grossouvre, B., Dos Reis, A. T., Gorini, C., and Nercessian, A., 2001, Structural geometry  
1164 in the eastern Pyrenees and western Gulf of Lion (Western Mediterranean): *Journal of Structural Geology*,  
1165 v. 23, p. 1701-1726.
- 1166 Mauffret, A., and Gorini, C., 1996, Structural style and geodynamic evolution of Camargue and Western Provençal  
1167 basin, southeastern France: *Tectonics*, v. 15, no. 2, p. 356-375.
- 1168 Miall, A. D., 1977, A review of the braided river depositional environment: *Earth-Science Reviews*, v. 13, p. 1-62.

- 1169 -, 1978, Facies types and vertical profile models in braided river deposits: A Summary, *in* Miall, A. D., ed., *Fluvial*  
 1170 *Sedimentology*, Volume Memoir 5, Canadian Society of Petroleum Geologists, p. 597-604.
- 1171 Mouthereau, F., Filleaudeau, P.-Y., Vacherat, A., Pik, R., Lacombe, O., Fellin, M. G., Castelltort, S., Christophoul,  
 1172 F., and Masini, E., 2014, Placing limits to shortening evolution in the Pyrenees: Role of margin architecture  
 1173 and implications for the Iberia/Europe convergence: *Tectonics*, v. 33, p. 2242-2314.
- 1174 Nemeč, W., and Postma, G., 1993, Quaternary alluvial fans in the southwestern Crete: Sedimentation processes  
 1175 and geomorphic evolution, *in* Marzo, M., and Puigdefabregas, C., eds., *Alluvial Sedimentation*, Volume  
 1176 Special Publication, 17, International Association of Sedimentologists, p. 235-276.
- 1177 Philip, H., Mattauer, M., Bodeur, Y., Séguret, M., Puech, J. P., and Mattei, J., 1978, Carte Géologique de la France  
 1178 au 1/50 000. Feuille de St Martin de Londres N°963: BRGM.
- 1179 Réhault, J. P., Boillot, G., and Mauffret, A., 1984, The western Mediterranean basin geological evolution: *Marine*  
 1180 *Geology*, v. 55, p. 447-477.
- 1181 Remy, J.-A., 2015, Les Périssodactyles (Mammalia) du gisement Bartonien supérieur de Robiac (Éocène moyen  
 1182 du Gard, Sud de la France): *Palaeovertebrata*, v. 23, no. 1-4, p. 211-216.
- 1183 Rémy, J.-A., 1985, Nouveaux gisements de Mammifères et Reptiles dans les Grès de Celas (Eocène sup. du  
 1184 Gard): *Palaeontographica*, v. 189, p. 171-225.
- 1185 Remy, J.-A., and Fournier, F., 2003, Mammifères fossiles des grès de Célas (Eocène supérieur du Gard):  
 1186 découvertes récentes: *Bulletin de la Société d'Etudes des Sciences Naturelles de Nîmes et du Gard*, v.  
 1187 64, p. 18-30.
- 1188 Rémy, J.-A., and Lesage, J.-L., 2005, Un nouveau gisement de vertébrés d'âge Priabonien et son contexte  
 1189 géologique (Tranchée de Nozières, Gard): *Bulletin de la Société d'Etudes des Sciences Naturelles de*  
 1190 *Nîmes et du Gard*, v. 65, p. 7-15.
- 1191 Rey, R., 1962, Sur l'importance paléontologique des faunes malacologiques continentales de très petites  
 1192 dimensions comme celles de la région de Montpellier: *C. R. Somm. Soc. Géol. France*, v. 10, p. 312-313.
- 1193 Reynaud, J.-Y., Dalrymple, R. W., Vennin, E., Parize, O., Besson, D., and Rubino, J. L., 2006, Topographic controls  
 1194 on production and deposition of tidal cool-water carbonates, Uzès Basin, SE France: *Journal of*  
 1195 *Sedimentary Research*, v. 76, p. 116-129.
- 1196 Romagny, A., Jolivet, L., Menant, A., Bessière, E., Maillard, A., Canva, A., and Gorini, C., 2020, Detailed tectonic  
 1197 reconstructions of the Western Mediterranean region for the last 35 Ma, insights on driving mechanisms:  
 1198 *Bulletin de la Société Géologique de France*, v. 191, p. art n° 37.
- 1199 Sanchis, E., 2000, Méthodologie d'imagerie 3D des bassins, des exemples dans le bassin du Sud Est: BRGM /  
 1200 Univ-Montpellier 2.
- 1201 Sanchis, E., and Séranne, M., 2000, Structural style and tectonic evolution of a polyphase extensional basin of the  
 1202 Gulf of Lion passive margin: the Tertiary Alès Basin, southern France: *Tectonophysics*, v. 322, p. 243-  
 1203 264.
- 1204 Séguret, M., and Benedicto, A., 1999, Le duplex à plis de propagation de rampes de Cazedarnes (arc de Saint-  
 1205 Chinian, avant-pays nord-pyrénéen, France): *Bulletin de la Société Géologique de France*, v. 170, no. 1,  
 1206 p. 31-44.
- 1207 Séguret, M., Benedicto, A., and Séranne, M., Structure profonde de la région du Gard Rhodanien - Apport du  
 1208 retraitement et de la réinterprétation de données sismiques régionales, *in* *Proceedings Journées*  
 1209 *Scientifiques Gard, Bagnols/Cèze (Gard), 1997, Volume Atlas des posters*, p. 31-32.
- 1210 Séranne, M., 1999, The Gulf of Lion continental margin (NW Mediterranean) revisited by IBS: an overview, *in*  
 1211 Durand, B., Jolivet, L., Horváth, F., and Séranne, M., eds., *The Mediterranean Basins : Tertiary extension*  
 1212 *within the Alpine Orogen*, Volume Special Publication 156: London, The Geological Society, p. 15-36.
- 1213 Séranne, M., Benedicto, A., Truffert, C., Pascal, G., and Labaume, P., 1995, Structural style and evolution of the  
 1214 Gulf of Lion Oligo-Miocene rifting : Role of the Pyrenean orogeny: *Marine and Petroleum Geology*, v. 12,  
 1215 p. 809-820.
- 1216 Serrano, O., and Hanot, F., 2005, Le bassin Oligo-Miocène de l'Hérault: un exemple de rétrocharriage des  
 1217 structures pyrénéennes. Implications hydrogéologiques: BRGM, BRGM/RP-53733-FR.
- 1218 Sigé, B., and Legendre, S., 1997, Un outil de la stratigraphie du Tertiaire continental : L'échelle de niveaux-repères  
 1219 de Mammifères *in* Aguilar, J. P., Legendre, S., and Michaux, J., eds., *Actes du congrès Biochrom'97*,  
 1220 Volume Mem.Trav. EPHE Inst. Montpellier 21, p. 47-54.
- 1221 Simons, D. B., Richardson, E. V., and Nordin, C. F., 1965, Sedimentary structures generated by flow in alluvial  
 1222 channels, *in* Middleton, G. V., ed., *Primary Sedimentary Structures and Their Hydrodynamic Interpretation*,  
 1223 Volume Special Publication 12, Society of Economic Paleontologists and Mineralogists, p. 34-52.

- 1224 Sissingh, W., 1998, Comparative Tertiary stratigraphy of the Rhine Graben, Bresse Graben and Molasse Basin:  
1225 correlation of Alpine foreland events: *Tectonophysics*, v. 300, p. 249-284.
- 1226 Southard, J. B., 1991, Experimental determination of bed-form stability: *Annual Review of Earth and Planetary*  
1227 *Sciences*, v. 19, p. 423-455.
- 1228 Teixell, A., Labaume, P., Ayarza, P., Espurt, N., de Saint Blanquat, M., and Lagabrielle, Y., 2018, Crustal structure  
1229 and evolution of the Pyrenean-Cantabrian belt: A review and new interpretations from recent concepts  
1230 and data: *Tectonophysics*, v. 724-725, p. 146-170.
- 1231 Teixell, A., Labaume, P., and Lagabrielle, Y., 2016, The crustal evolution of the west-central Pyrenees revisited:  
1232 Inferences from a new kinematic scenario: *Comptes Rendus Géosciences*, v. 348, no. 3-4, p. 257-267.
- 1233 Ternois, S., Odum, M., Ford, M., Pik, R., Stockli, D., Tibari, B., Vacherat, A., and Bernard, V., 2019,  
1234 Thermochemical Evidence of Early Orogenesis, Eastern Pyrenees, France: *Tectonics*, v. 38, no. 4,  
1235 p. 1308-1336.
- 1236 Thaler, L., 1962, Premiers résultats d'une recherche systématique des dents de Rongeurs, par lavage de marnes  
1237 de l'Oligocène, en Bas-Languedoc: *C. R. Somm. Soc. Géol. France*, v. 10, p. 315-316.
- 1238 Tugend, J., Manatschal, G., Kuszniir, N. J., Masini, E., Mohn, G., and Thion, I., 2014, Formation and deformation  
1239 of hyperextended rift systems: Insights from rift domain mapping in the Bay of Biscay-Pyrenees: *Tectonics*,  
1240 v. 33, p. 1239-1276.
- 1241 Vandenberghe, N., Hilgen, F. J., and Speijer, R. P., 2012, The Paleogene Period, *in* Gradstein, F. M., Ogg, J. G.,  
1242 Schmitz, M. D., and Ogg, G., eds., *The Geologic Time Scale 2012, Volume 2*, Elsevier, p. 855-821.
- 1243 Vergés, J., and Garcia-Senz, J., 2001, Mesozoic evolution and Cainozoic inversion of the Pyrenean Rift, *in* Ziegler,  
1244 P. A., Cavazza, W., Robertson, A. H. F., and Crasquin-Sleau, S., eds., *Peri-Tethys rift / wrench basins*  
1245 *and passive margins, Volume Mémoire 186: Paris, Muséum National d'Histoire Naturelle* p. 187-212.
- 1246 Viillard, P., 1987, Un modèle de charriage épi-égyptique: la nappe des Corbières orientales (Aude, France): *Bulletin*  
1247 *de la Société Géologique de France*, v. III, no. 3, p. 551-559.
- 1248 Ziegler, P. A., and Dèzes, P., 2005, Evolution of the lithosphere in the area of the Rhine Rift System: *International*  
1249 *Journal of Earth Sciences*, v. 94, p. 594-614.
- 1250